'The Northern Lights have seen queer sights.....!

The Cremation of Sam McGee, by Robert Service

UNIVERSITY OF ALBERTA AT CALGARY

'AURORAL PHOTOGRAPHY USING A MECHANICAL FLYING SPOT SCANNER'

by

G. R. PILKINGTON

A THESIS

SUBMITTED TO THE FACULTY OF GRADUATE STUDIES

IN PARTIAL FULFILLMENT OF THE REQUIREMENTS FOR THE DEGREE

OF MASTER OF SCIENCE

DEPARTMENT OF PHYSICS

CALGARY, ALBERTA

APRIL 1965

© G.R. Pilkington 1971

A B S T R A C T

A survey of devices suitable for producing photographs of low intensity aurora was made.

A mechanical flying spot scanner was designed and constructed to take fast moving photographs of low intensity aurora. This device was used to study the correlation between visible aurora and x-rays detected at balloon altitudes. From this analysis a close association was noted between these phenomena for the particular auroral display considered.

ACKNOWLEDGEMENTS

The author would like to thank Dr. C. D. Anger, of the Physics Department, University of Alberta, Calgary, who supervised this research. He furthermore acknowledges with gratitude the support and suggestions of Dr. T. A. Clark also of the Physics Department.

Mr. C. Hansen and Mr. D. Will of the Physics Department assisted with the electronics, and Mr. W. A. Jones and staff of the Physics Workshop helped in the construction of the mechanical parts of the scanner.

The use of facilities and assistance provided by Dr. J. H. Brandy and the staff of the Defence Research Northern Laboratory and the Churchill Research Range, Churchill, Manitoba is also greatly appreciated.

Thanks are due also to the University of Alberta and the National Research Council of Canada for their support of this research in the form of Graduate Teaching Assistantships and summer research grants, respectively.

TABLE OF CONTENTS

LIST OF ILLUSTRATIONS

List of Illustrations

CHAPTER 1

INTRODUCTION AND AURORAL PHENOMENA

It is difficult, if not impossible, to obtain fast time correlations between visible aurora and related phenomena without fast, moving photographs of the aurora over large regions of the sky.

The various instruments and techniques which can be used to obtain photographs of the aurora will be described in the following chapter. Photometers and verbal descriptions may also be used to provide information on auroral intensity variations.

Photometers indicate only the average light intensity within their field of view, and so would produce the same signal for a small bright source as for a large faint source. Verbal descriptions of the aurora recorded on magnetic tape (a technique used extensively by the auroral group at U.A.C.) is limited due to the complexity and rapidity of the auroral

motions as well as numerous human limitations (see Chapter 4.)

This thesis describes an apparatus for taking fast moving photographs of low intensity aurora. The instrument was designed to have the following characteristics:

(a) capable of up to 10 pictures per second

(b) 120^{o} x 120^{o} field of view

(c) 1.2^{o} x 1.2^{o} resolution

(d) sufficiently sensitive to detect Brightness I Aurora (see Chapter 2).

When constructed, the apparatus was found to have substantially less than the designed sensitivity due to the low reflectivity of the mirrors, which was not adequately taken into account in the calculations. The device still represented a considerable improvement over direct photography.

The apparatus was in operation during the test flight of a balloon-borne x-ray detector which employed a new type of telemetry system (see Appendix). An attempt

has been made to correlate the x-rays detected by the balloon equipment with auroral photographs obtained by means of the apparatus. Variations in the x-ray energy spectrum with position and intensity of the aurora will also be discussed.

Auroral Phenomena and X-Rays

Auroral light comes mainly from ionospheric atoms and molecules, especially those of oxygen and nitrogen, which are excited and ionized by primary particles, mainly electrons, but also protons. The particles descend along the geomagnetic lines of force and enter the atmosphere primarily in zones centered about the magnetic poles, at geomagnetic latitudes of about 65° in the northern and southern hemispheres.

The electrons directly associated with the aurora generally have energies of a few KeV, but a significant number of electrons with energies up to 100 KeV or higher

may be present (O'Brien and Taylor, 1964).

It is generally believed that the particles producing the visible aurora are locally accelerated by a mechanism influenced by the solar wind--a continuous flow of neutral but ionized hydrogen gas, which comes from the sun. Chapman (1961) suggested that the wind may set up an electric current round the earth on the equatorial plane, which affects the electrons trapped in the Van Allen radiation belts, causing them to be precipitated into the atmosphere.

The electrons that enter the upper atmosphere lose most of their energy producing ionization and excitation of the gas atoms at altitudes in the vicinity of 100 km. Higher energy electrons also give up a small part of their energy in producing bremsstrahlung x-rays, which penetrate down to 30 km where they can be detected by balloon borne equipment.

X-rays with energies less than 30 KeV are predominantly photoelectrically absorbed. X-rays with energies greater than 30 KeV are predominantly Compton scattered.

These x-rays lose some energy with each scatter. In addition, because these x-rays do not travel directly from the source to the detector, they increase their chance of being photoelectrically absorbed before reaching the detector.

The electrons which are directly associated with visible aurora produce x-rays which have a high probability of being photoelectrically absorbed before penetrating down to balloon altitudes. The x-rays which do reach balloon altitudes are scattered many times and so give little indication of their original direction.

Experimental Evidence

A direct association between x-rays and visible aurora was found in balloon experiments over Minneapolis (Winkler and Peterson, 1957; Winkler et al., 1958 and 1959).

Anderson and Dewitt (1963), in balloon experiments over College, Alaska, also found a very close minute-by-minute correlation between x-ray intensity and auroral

luminosity. They determined the auroral intensity at the 100 km height above the balloon from All-Sky Camera photo-photographs (see Chapter 2, Section (i)). Anderson thus concluded that on this particular occasion the electrons associated with aurora produce a measurable number of x-rays at balloon altitudes.

Contrary to these results Anderson (1958 and 1961), from balloon experiments over Fort Churchill, Manitoba, and Fairbanks, Alaska, concluded that x-rays were not always associated with visible aurora. He reported that on numerous occasions high x-ray count rates were observed with no sign of visible aurora, and that on other occasions aurora was observed without x-rays.

Anderson suggested that the acceleration of electrons in the atmosphere might be a common phenomenon which was accompanied by optical aurora only on special occasions. He also suggested that perhaps other conditions had to be met before optical aurora were produced, for example, the

presence of protons.

It seems to be generally accepted that a correlation exists between visible aurora and x-rays outside the auroral zones, but not necessarily inside. However, it should be mentioned that, in spite of very extensive studies of auroral x-ray phenomena by numerous investigators, only on very few occasions have balloon flights been carried out under conditions where simultaneous auroral observations could be made. Even when correlations were possible, the only optical data available has been All-Sky Camera pictures or brief visual reports, neither of which provides very good time resolution.

CHAPTER 2

AURORAL ILLUMINATION AND AURORAL PHOTOGRAPHY

The major difficulty in obtaining pictures of the aurora arises from its extremely faint luminosity.

The Brightness Index is a visual estimate of the order of magnitude of auroral intensities. It is given in terms of an apparent isotropic emission rate of 10^6 photons per second from a column of aurora in the observer's line of sight and of one square centimeter area. This unit is the Rayleigh.

For the green oxygen emission 5577 Å a scale of intensity index is defined by the following:

Intensity (5577 Å) Kilo-Rayleighs (IkR = 1000 Rayleighs)	Scene Brightness (lumens per sq. ft.)	Intensity Index	Remarks on visual appearance of typical aurora
0.1	2×10^{-5}	0	Subvisual
1	2×10^{-4}	I	Comparable to Milky Way. No color perceived.
10	2×10^{-3}	II	Comparable with moonlit cirrus cloud. Color (green) sometimes perceived.

(table cont'd.)

Intensity (5577 Å) Kilo-Rayleighs (IkR = 1000 Rayleighs)	Scene Brightness (lumens per sq. ft.)	Intensity Index	Remarks on visual appearance of typical aurora
100	2×10^{-2}	III	Comparable with brightly moonlit cirrus cloud or moonlit cumulus cloud. Color perceived.
1000	2×10^{-1}	IV	Much brighter than 3. Sometimes casts easily discernible shadows.

From the International Auroral Atlas. Published for the International Union of Geodesy and Geophysics.

It is interesting to consider the sensitivity of the human eye. According to A. Morton (1964) a young trained observer begins to be able to see at an illumination of about 10^{-5} ft. candles. (This corresponds to a scene brightness of 10^{-5} lumens per sq. ft. assuming 100% reflectivity of the scene.) At this level he sees only large high-contrast objects. If the illumination is increased to 10^{-2} ft. candles, about equivalent to the illumination produced by the full moon, it is possible to make out large newsprint but still not possible to discern color. Color can be discerned with an illumination of 10^{-1} ft. candles.

Thus an observer can easily detect a source of light of luminance similar to that of a brightness one aurora; however, the problem of contrast must be considered. The clear night sky is equivalent to a scene brightness of 10^{-4} lumens per sq. ft. (one half that of a brightness I aurora). Thus to detect low intensity aurora it is desirable to reject the sky light and any other sources of light that could enter the detector. Auroral emission lines have bandwidths of typically 0.01 Å, thus the required rejection of unwanted light can be effected by incorporating in the detector a light filter with a narrow transmission bandwidth.

Thin film interference filters provide a narrow transmission bandwidth, with about 60% transmission efficiency at the transmitted wavelength. These filters have the property that the wavelength of the transmitted light depends on the angle at which the light is incident on the filter. Thus if the light beam incident on the filter is not sufficiently well-collimated, the transmission

bandwidth of the filter will be broadened, giving poorer rejection of unwanted light and decreased transmission of the desired wavelength. It is necessary to consider this in the discussion of the suitability of a particular device as an auroral detector.

The various methods of producing a picture of the aurora will now be considered in detail, the sensitivity and merits of the methods will be discussed.

The methods available are:

(i) Direct photography using photochemicals,

(ii) Scanning techniques including (a) mechanical and (b) electronic,

(iii) Image intensification utilizing various types of electron multiplication.

(i) DIRECT PHOTOGRAPHY

The first auroral photographs were taken by Brendel in 1892. Photographs attempted prior to this date

failed due to insufficiently sensitive plates and lenses. Brendel used an f/3.5 lens (see calculations at end of this section) and sensitive orthochromatic plates and succeeded in photographing a bright band with an exposure of seven seconds.

In 1909, Carl Stormer began experimenting with photographic techniques and built a camera using an f/2.0 lens and sensitive photographic plates, with which he was able to photograph bright auroral forms with exposure times of one-half second. He was able to photograph all auroral forms except flaming and pulsating aurora. These two forms are generally of Brightness I or II. Stormer applied these techniques to height finding of the aurora by triangulation.

In 1913 Stormer attempted moving photographs of the aurora using a camera incorporating an f/3.5 lens. With this equipment he was able to detect bright aurora with an exposure of 4 seconds.

Gartlein (1947) developed the All Sky Camera.

The camera consists of a normal motion-picture camera mounted above a convex spherical mirror.

This camera is generally used for indicating the presence of aurora only where space and time resolution are not too important. The picture produced by this camera is extremely distorted, so elevation angles are often indicated by small lights attached to the framework supporting the film camera (see Chapter 4 for examples of A.S.C. photographs).

Several All Sky Cameras have been built similar to the camera described above but with optical elements to reduce distortion (Struve, 1951, and Lebedinski, 1955).

The All Sky Camera is generally used for patrol work on auroral occurrence. The camera takes a photograph of the sky every minute throughout the night with an exposure time of about 20 seconds. This exposure is found to be adequate to record all auroral intensities.

To improve the time response of the camera, Montalbetti (1957) incorporated an f/0.71 lens in the film camera, and so was able to take moving photographs of

pulsating and flaming aurora at one frame per second (exposure of about 0.6 seconds). These were of intensity II to III on the auroral intensity index (private communication).

It is essential for an auroral detector to have a wide field of view because of the large angular extent of visible aurora. The detector must also incorporate few optical elements in order to maintain maximum optical efficiency. The most convenient way of satisfying these two requirements is to use a convex mirror as used in the All Sky Camera. At no point in a wide angle lens or A.S.C. system is all the light parallel, and so a narrow bandwidth interference filter cannot be incorporated in either of these systems with maximum efficiency. In an A.S.C., for example, the filter could be placed between the mirror and film camera, and in this position would intercept light converging at an angle of about 20 degrees. Increasing the distance between mirror and camera would decrease the angle. This would necessitate a longer focal length lens in the film camera. To maintain the

speed of the optical system, a larger aperture lens would be necessary, which would require a correspondingly larger interference filter. It is necessary that the bandwidth of the interference filter is sufficiently wide that auroral light from all regions of the sky passes unimpeded, despite the different angles at which the light is incident upon the filter. For the usual A.S.C. a filter with a bandwidth of about 200Å would be required. With photographic techniques it is impossible to combine maximum sensitivity and a wide angular field of view with good background light rejection, unless a very large diameter interference filter is available

Sensitivity of Photographic Materials

The sensitivity of photographic materials will now be considered from the point of view of taking high speed moving photographs of the aurora. The exposure time required to produce a photograph of a Brightness I aurora will be calculated.

At normal light levels (i.e. daylight) a given

exposure--product of exposure time and light intensity--produces a given film density after development. This reciprocity law breaks down at extremely low and extremely high light levels. At these two extremes, a larger exposure than suggested by the reciprocity law is required to produce a given film density.

Graphs are provided by film manufacturers showing the exposure required for a given light intensity to produce a detectable film density.

An aurora emitting N photons/cm^2 (col) sec produces a surface illumination, i, of

$$i = \frac{N}{4\pi} \text{ photons/cm}^2 \text{ sterad sec.}$$

For a detector with an area of A cm^2 and angular field of view Ω steradians.

The number of photons/sec incident on the detector

$$i' = \frac{NA\Omega}{4\pi} \text{ photons/sec.}$$

For a film of area a cm^2, the number of photons/cm^2 sec incident on the film (assuming all photons incident on

detector are transferred to the film) is

$$n = \frac{NA\Omega}{4\pi a} \text{ photons/cm}^2 \text{ sec.}$$

The "speed" of a lens is given as an 'f' number or ratio. f ratio = F/d

where F is the focal length of the lens, and

d its diameter.

Area of lens $A = \frac{\pi d^2}{4}$

and angular field of view $\Omega = \frac{a}{F^2}$.

Thus, $\frac{A\Omega}{\pi a} = \frac{1}{4f^2}$

or $$n = \frac{N}{16f^2} \text{ photons/cm}^2 \text{ sec.}$$

On converting this to an illumination 'I' on the film, taking 1 photon/sec = 2.2×10^{-16} lumens for green light (5577 $\mathring{A}$)

$$I = \frac{N(2.54 \times 12)^2 \, 2.2 \times 10^{-16}}{16f^2}$$

$$= \frac{N(1.25 \times 10^{-14})}{f^2} \text{ lumens/sq. ft. or ft. candles.}$$

For Brightness I aurora $N = 10^9$, and assuming f = 1

this gives $I = 1.25 \times 10^{-5}$ ft. candles

or 1.25×10^{-4} meter candles.

Using the reciprocity curves for the most sensitive films available, eg., Kodak Record X (ASA 1600) an exposure time of about 50 seconds would be required to produce an image on the film, corresponding to a film density of 0.3 above the basic fog level of the film--this is equivalent to a signal to noise ratio of one. Since such a film density is not required for this minimum intensity aurora, an exposure time of about 20 seconds is found to be adequate.

Using the very fastest lenses available (f ratio of 0.5) and pre-exposing and postexposing the film, this exposure time of 50 sec could be reduced by a factor of about 10.

Film sensitivity is basically limited by the fact that with present emulsions an average of about 10 photons per grain are required to make the grain developable, and, in addition, all these photons must be absorbed by the grain

within a short period of time (failure to comply to this latter condition results in low light level reciprocity failure). If the size of the silver halide grain could be increased without loss of sensitivity, then, for a particular light intensity, more photons would be incident on each grain. With some emulsions it seems likely that the grain size could be increased without too great a loss of grain sensitivity (G. C. Farnell and J. B. Chanter, 1961). Unfortunately, film manufacturers are reluctant to sacrifice picture resolution for the sake of sensitivity.

Film is very well adapted for high resolution pictures, and when considerable picture detail is required it is superior to any other picture imaging device . However, present emulsions are not sufficiently sensitive to take fast moving photographs of low intensity aurora, and unless resolution can be sacrificed for sensitivity, it seems unlikely that an emulsion will be developed suitable for this application.

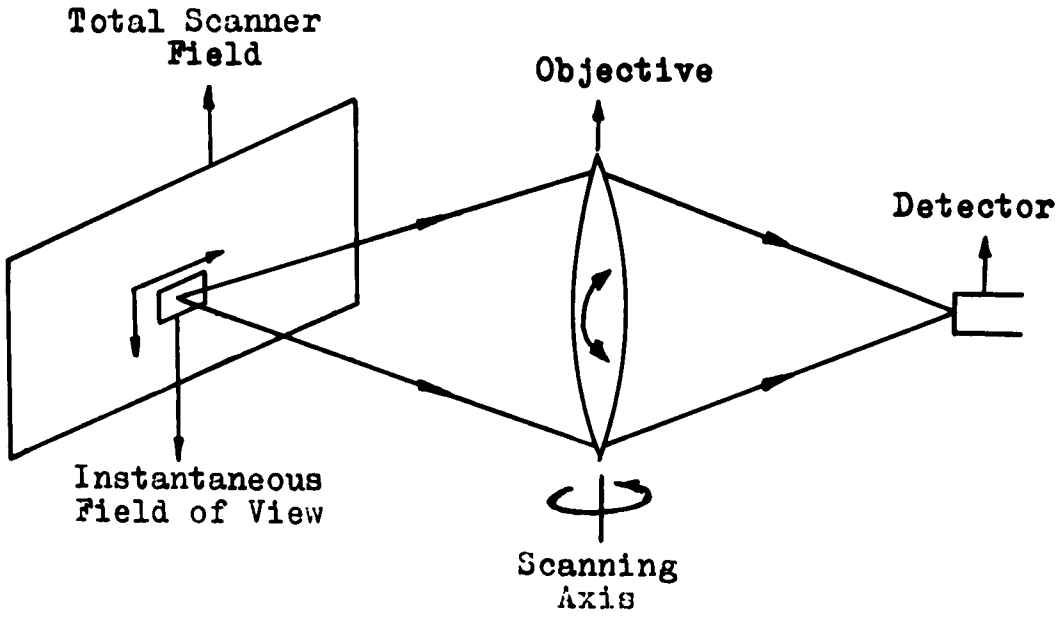

Fig. 1(a): Scanning Spot System

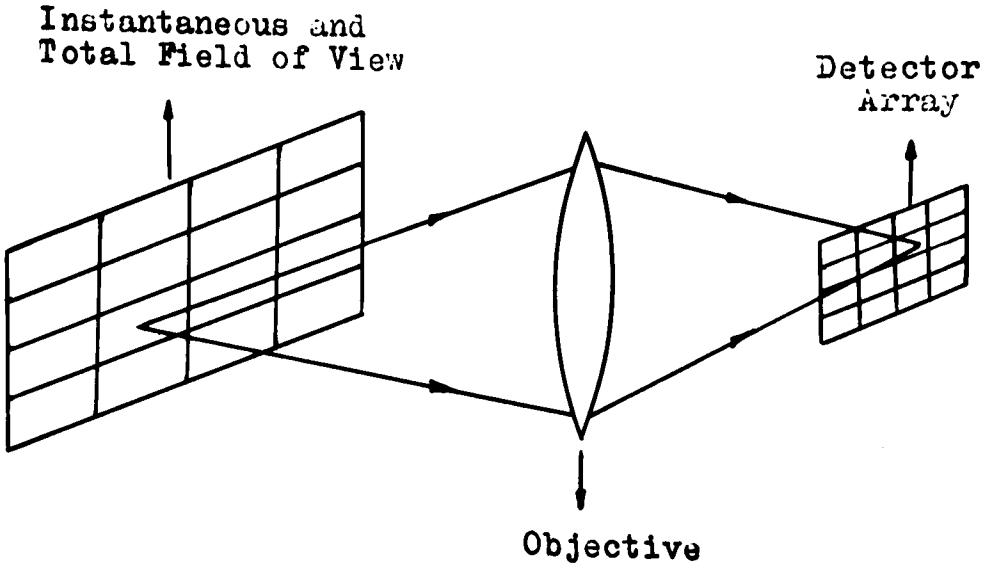

Fig. 1(b): Mosaic System

(ii) SCANNING DEVICES

Various scanning techniques lend themselves to the production of high speed pictures at low light levels. These involve dissecting the picture into a large number of parts or elements and systematically sampling the light from each element by means of a detector. This sequential sampling or scanning can be effected either mechanically or electronically.

The scanner can either sample the original picture (object plane scanning) or an image of the picture (image plane scanning). The latter method is generally simpler but first requires a good quality image of the picture, which is difficult to obtain if a large angular field of view is required.

Mechanical scanning can be achieved by Flying Spot Scanning (Fig. 1(a)). In this method the detector is directed systematically to each element of the dissected picture. The detector thus receives light from each part

of the picture for only a small fraction of the total time required to scan the whole picture. This is basically very inefficient; however, this inefficiency can be reduced at least in part by using a large detector. The system is simple electronically requiring only one detector. An important feature of the object-plane flying spot scanner is that it lends itself readily to the incorporation of a narrow band interference filter, as the light incident on the detector comes from a very small area of the object and so only converges at a very small angle. Electronic scanning (Mosaic scanning, Fig. 1(b)) provides much greater sensitivity than Flying Spot Scanning. The detector consists of a two-dimensional array of light sensors. Each sensor looks continuously at one small part of the object and the light from the particular part of the object accumulates in the sensor. The signal on each sensor, produced by the accumulated light, is sampled when the sensors are electronically scanned.

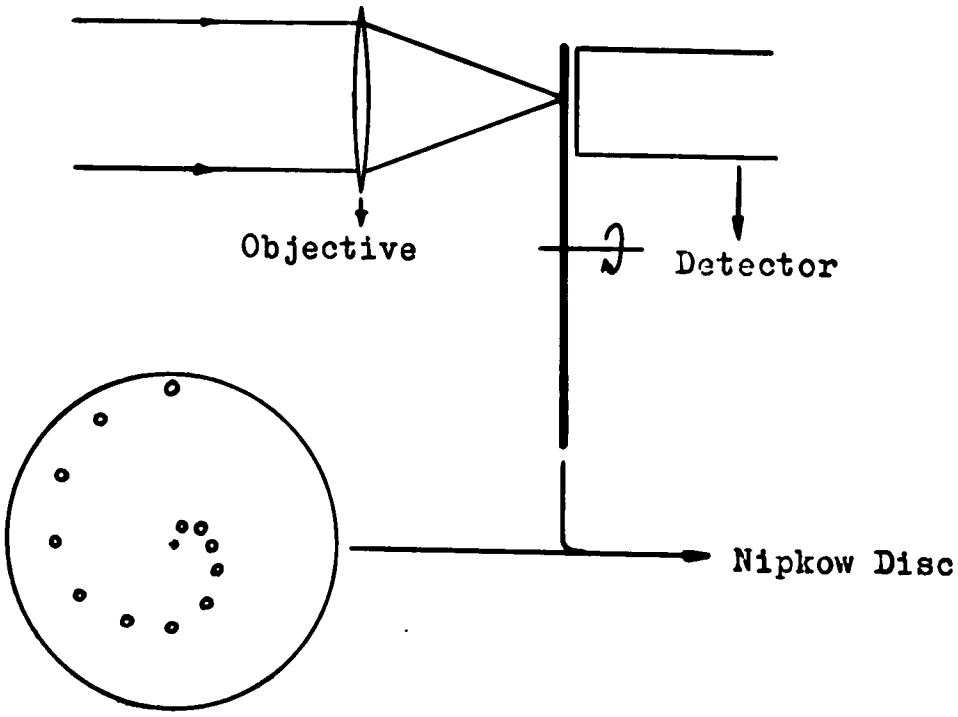

Fig. 2: Nipkow Disc

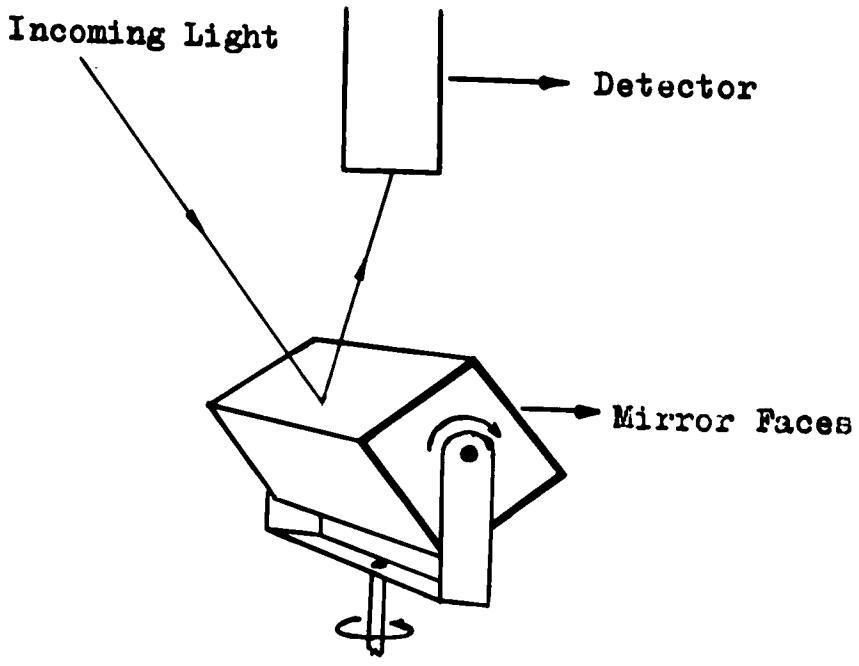

Fig. 3: Spiral Scanner

(a) Mechanical Scanning Devices

Many methods are available for obtaining a flying spot scan (Holten and Wolfe, 1959, and McFee, 1959). The Nipkow Disc system, which was one of the first techniques used in television, uses image plane scanning (Fig. 2). A lens system forms an image on the disc. The holes in the Nipkow disc spiral in towards the center of the disc. As the disc rotates each consecutive hole scans over a different part of the image. The light passing through the holes falls onto the detector.

A Nipkow disc scanner was constructed by the author. Because of the extremely large angular field of view required, the angular resolution obtainable with the simple disc described above was inadequate. This problem was overcome by designing the scanner so that one rotation of the disc scanned only one-quarter of the image, and four rotations of the disc scanned over the whole image, thus increasing the resolution by a factor of four. The light which passed through the holes fell onto a photomultiplier.

The current produced by the photomultiplier was used to intensity modulate the beam of an oscilloscope made to scan the scope screen in synchronism with the rotation of the scanning disc.

The idea was rejected mainly because of the precision required in making the Nipkow disc and the optical difficulties in making the system operate with a narrow interference filter while still retaining a large light collecting area and angular field of view.

Object plane flying spot scanning

The simplest way of producing this scan is by monitoring, by means of a fixed detector, the light reflected off a plane mirror which is rotating about two perpendicular axes simultaneously. The relative angular velocity about each axis determines the scan pattern.

Fig. 3 shows a scanner of this type built by Dr. C. D. Anger. A cube, with top, bottom and opposite two

sides aluminised, rotates about a vertical axis and also about a horizontal axis (the horizontal axis rotates with the mirror assembly about the vertical axis). If the angular velocity about the vertical axis is much greater than that about the horizontal axis the scan pattern is a spiral, centered about the zenith. If the angular velocity of the cube about the horizontal axis is much greater than that about the vertical axis the scan pattern will be radial (similar to a radar scan).

The scanner constructed was of the former type using a spiral scan pattern. Light from a small area of the sky is reflected off one mirror face onto the detector. As the mirror rotates about a vertical axis, the detector sees the periphery of a circle in the sky centered about the zenith. As the mirror rotates slowly about a horizontal axis the circle changes its elevation, and so in one complete scan the detector is directed systematically over the entire sky.

Another method using a single mirror is used in aircraft reconnaisance. The rotating mirror provides the N-S (say) scan line, whilst the motion of the aircraft provides the E-W scan of a rectangular scan pattern. A scanner of this type has been constructed by Dr. C. D. Anger to be flown in a rocket. In the rocket scanner the fast rotating mirror provides the vertical scan in line with the rocket's axis and motion, and the slow rotation of the rocket the horizontal scan. This produces a "barrel" scan pattern.

The scanner described in this thesis employs a rectilinear scan, effected by two separate moving mirrors. The characteristics of this system are described in the next chapter.

This particular system was chosen as it appeared to be the simplest method of achieving a wide field of view, reasonable space resolution, fast scan rate, simple reproduction of the scan pattern and simple synchronisation between scanner and reproduced picture. Also the system has a large

light accepting area and is reasonably versatile to different scanning rates and changes in angular resolution. The sensitivity of this type of scanner will now be calculated.

Sensitivity of Mechanical Scanner

An aurora emitting N photons cm^{-2}(column) sec^{-1} would produce a surface illumination of

$\frac{N}{4\pi}$ photons cm^{-2} $steradian^{-1}$ sec^{-1}.

This illumination will produce n photoelectrons per second from the scanner photomultiplier photocathode,

where $n = \frac{NA\emptyset}{4\pi} \epsilon E$ photoelectrons sec^{-1}

where A is the light-receiving area of scanner (25 cm^2)

$\emptyset$ is the solid angle subtended by each picture element ($(\frac{1.2}{57})^2$ sterads) for 1.2^o angular resolution)

E is the optical efficiency of the scanner (10%), and

ϵ is the quantum-efficiency of the photocathode (5%).

For a Brightness I aurora $N = 10^9$

$$n = \frac{10^9 \times 25}{4\pi} \left(\frac{1.2}{57}\right)^2 \times 0.1 \times 0.05 \text{ photoelectrons/sec}$$

$$= 4.4 \times 10^3 \text{ photoelectrons sec}^{-1}.$$

For an EMI 9514S photomultiplier the dark current = 10^{-10} amp. This corresponds to about 10 photoelectrons sec^{-1}.

Thus the signal produced by a Brightness I aurora is about 4×10^2 greater than the dark current noise signal.

From this analysis a Brightness I aurora over the whole sky produces 4×10^3 spots per seconds, for a picture containing 10^4 picture elements. Thus if a patch of Brightness I aurora occupies an area of the sky, the corresponding area of the oscilloscope screen will contain a single spot in 40% of the relevant picture elements for an exposure time of one second, or 4% of the picture elements for an exposure of 1/10 second. Each picture element has been designed to accept about 50 spots, thus increasing the

dynamic range of the system. A Brightness II aurora, producing 4 x 10^4 spots per second, will appear as 4 spots per picture element per second, and a Brightness III aurora as 40 spots per picture element per second.

As can be seen from this analysis, the limitation of the scanner at short exposure times and low auroral intensities is the low picture resolution, due to the inadequate number of photoelectrons produced in each scan at auroral intensities. The signal, however, is substantially higher than the noise level, and the signal to noise ratio remains constant with decrease or increase of the picture scan time. An increase of sensitivity can be obtained by intergrating the light received over many scans.

The above analysis assumes amplification of the signal by pulse amplifiers, with a 0.1 microsecond time response and sufficiently high gain to amplify a single photoelectron pulse from the photomultiplier to produce a recordable spot on the oscilloscope screen. The photographs shown

in this thesis were obtained using direct coupled amplifiers. Low intensity aurora produced a few individual spots, corresponding to the larger photomultiplier pulses (see Fig. 14). Bright aurora produced continuous brightening of the screen, because of the relatively long time constant of the amplifier. The d.c. amplifier has since been changed to a high gain pulse amplifier. The system is more sensitive than before but still not as sensitive as calculated above, due mainly to the amplifier gain, which is insufficient to produce a recordable spot from all single photoelectron pulses.

For a single scan, brightness tones are indicated by varying densities of spots in different areas of the screen. The sensitivity of the instrument is adjusted such that bright aurora just produces a continuous brightening of the screen.

If, however, a large number of consecutive, single, fast scans are photographed on one film frame the scanner sensitivity can be increased, without reduction of the

detectable brightness range. The brightest aurora will now no longer flood the oscilloscope screen on each scan, but over the period of time accumulate more light on the film than the dim aurora. Brightness tones will now be given by variations in the film density, although faint aurora may still appear as individual spots of light depending on the scanner sensitivity and the total film exposure time.

(b) Electronic Scanning Devices

These devices work on the principle described at the beginning of this section. A lens system is used to focus an image of the aurora onto the detectors and so the problems regarding the use of a narrow band interference filter are similar to those discussed in Section (i) of this chapter.

There are two basic types of electronic scanning devices:

(1) The Vidicon -- most sensitive versions respond to a minimum photocathode illumination of 10^{-1} ft. candles, and

(2) The Image Orthicon -- sensitive to a minimum photocathode illumination of 10^{-7} ft. candles.

The Vidicon is not sensitive enough to detect Brightness I aurora (equivalent to a photocathode illumination of 10^{-5} ft. candles) although experimental versions, using secondary electron conduction amplification and capable of integrating over long times, are sensitive to 10^{-4} ft. candles (Goetze and Boerio, 1964).

Sensitivity of the Image Orthicon

From manufacturers specifications a photocathode illumination of 10^{-5} ft. candles, corresponding to a Brightness I aurora, could be reproduced with a resolution of about 300 lines per target inch at 30 pictures per second. The angular resolution for a photocathode of

$1\frac{1}{3}$ inch x $1\frac{1}{3}$ inch useful area, would be $\frac{\Omega}{(400)^2}$ steradians, where Ω is the angular field of view of the system in steradians.

The maximum sensitivity of the image orthicon can be improved by reducing the resolution or increasing the time between consecutive picture scans and so allowing the light to accumulate on the detectors for a longer time.

The lowest light level detectable is set by the shot noise level of the tube, equivalent to about 10^{-9} amps. This restricts the lowest detectable light level to about 10^{-7} ft. candles, a factor of about 10^2 lower than Brightness I aurora. At these light levels the picture resolution must be reduced to about 140 lines per picture. This corresponds to a resolution of about 1.3° x 1.3° for a field of view of 2π steradians, which is still adequate to distinguish most forms of aurora.

The image produced by these devices is on a remote cathode ray tube viewing system. The signal from the detector can be amplified sufficiently so that the final image is

bright enough to be photographed for permanent record.

(iii) Electronic Image Intensifiers

In these devices a lens produces an image of the aurora on a photosensitive cathode. Electrons given off by the light incident on the cathode are multiplied over several stages by transmission secondary emission or phosphor/photocathode electron amplification. The electrons then fall onto a phosphorescent screen, where the image is reproduced several orders of magnitude brighter. This image can be photographed directly.

As a lens is used to produce an image of the aurora, the problems involved in using a narrow band interference filter, for the rejection of background light, are again similar to those discussed in Section (i) of this chapter.

Sensitivity of Image Intensifier

A Brightness I aurora produces a photocathode illumination of 10^{-5} ft. candles.

The light gain of an image intensifier is generally about 2×10^5. Thus, a photocathode illumination of 10^{-5} ft. candles results in an image on the phosphor of brightness 2 lumens/sq. ft.

If an f/1 lens is used to focus this image onto film, the resulting film illumination will be about 0.1 ft. candles. This light level can be recorded by a high speed film with an exposure time of about 1/50 second.

The space resolution of an image intensifier is usually about 200 line pairs per millimeter, i.e. resolution is sufficient to distinguish two lines separated by 1/200 mm on the photocathode; however, the best lens available will only resolve 100 line pairs. For a photocathode with a sensitive area of 2" x 2", the angular resolution = $\Omega/(5 \times 10^3)^2$ steradians, where Ω is the angular field of view of the system in steradians.

The dark noise of the image intensifier (spurious emission of photoelectrons from the photocathode) is not significant, except at photocathode illuminations of

about 10^{-9} ft. candles.

At about 10^{-8} ft. candles, however, the picture resolution for short exposure times has greatly deteriorated due to insufficient photons falling on the photocathode.

Intensifier Orthicon and Vidicon Combinations

Either of the two electronic scanning devices considered in Section (ii)b can be combined with the image intensifier. The result of such a combination is a system with the sensitivity of the intensifier and a remote picture display screen. The latter is an almost essential requirement for places in the auroral zone due to climatic conditions.

Comparison of the Sensitivities and Practical Applicability of the Various Techniques Considered

In this section the sensitivity of the various techniques considered will be compared with that of the scanner described in this thesis. The usefulness of the devices will be considered for the particular application of

auroral photography, and the advantages and disadvantages of the devices will be discussed.

Table Showing a Comparison of the Devices Considered.

Detector	Total Angular Field of View (Sterads)	Angular Resolution (Sterads)	Exposure* Time for BI Aurora (secs)
Scanner	4.4	4×10^{-4} 8×10^{-2}	1 1/10
Film	(a) 2π (b) 1/4	3×10^{-7} 1×10^{-8}	20 20
Image Orthicon	(a) 2π (b) 1/4	20×10^{-6} 10×10^{-7}	1/30 1/30
Image Intensifier	(a) 2π (b) 1/4	3×10^{-7} 1×10^{-8}	1/30 1/30

* The exposure time quoted is that required to produce a permanent picture on film.

(a) Using the detector in conjunction with an All Sky camera mirror.

(b) Using narrow angle lens.

The simplest system of those considered is direct filming of the aurora. Unfortunately this system is not sufficiently sensitive to produce fast moving photographs of dim aurora.

The image intensifier used with an All Sky Camera mirror was considered to be the best system of those discussed. It is the most sensitive of the systems and provides a final picture at auroral light levels of similar quality to that obtained by film alone. The image intensifier appears superior to the image orthicon in simplicity, dynamic range of intensities for a particular sensitivity setting and cost.

The image orthicon has many drawbacks--complexity, criticality of settings and cost. Unlike the previous two systems considered, the image orthicon requires a display system on which the picture is reproduced for photographing. This increases the complexity of the system, although remote viewing is often essential.

The mechanical scanner is basically the least efficient of the devices considered. For a total exposure time of 1 second the equivalent exposure time per picture element is 10^{-4} seconds. This figure could be increased by increasing the number of detectors used but this would

greatly increase the complexity of the device.

Although the resolution of the scanner is much worse than that of the other systems considered, it is sufficient for showing the gross features of most types of aurora. However, it is not good enough to show such detail as fine ray structure in auroral forms.

The sensitivity of the scanner can be improved, without deterioration of the picture quality, by increasing the light receiving area. This is limited only by mechanical problems and in theory a mechanical scanner could be made as sensitive as an electronic scanner. One serious inefficiency of the present device results from the poor reflectivity of the mirrors.

If the problem is not one of detecting the low auroral intensities, but of rejecting background light, e.g. photographing twilight aurora, only the flying spot scanner can provide the desired wide angular field of view and give adequate rejection of background light. In fact the flying

spot scanner can provide the maximum possible rejection of background light that can be obtained with an interference filter, and in this respect it is superior to the other devices considered.

The image orthicon system has been used for auroral photography and found to be capable of producing high resolution photographs of Brightness I aurora at 24 frames per second (Davis and Hicks, 1964 and 1965). A complete discussion of the use of this device for auroral photography is given by Spalding and Anderson (1963).

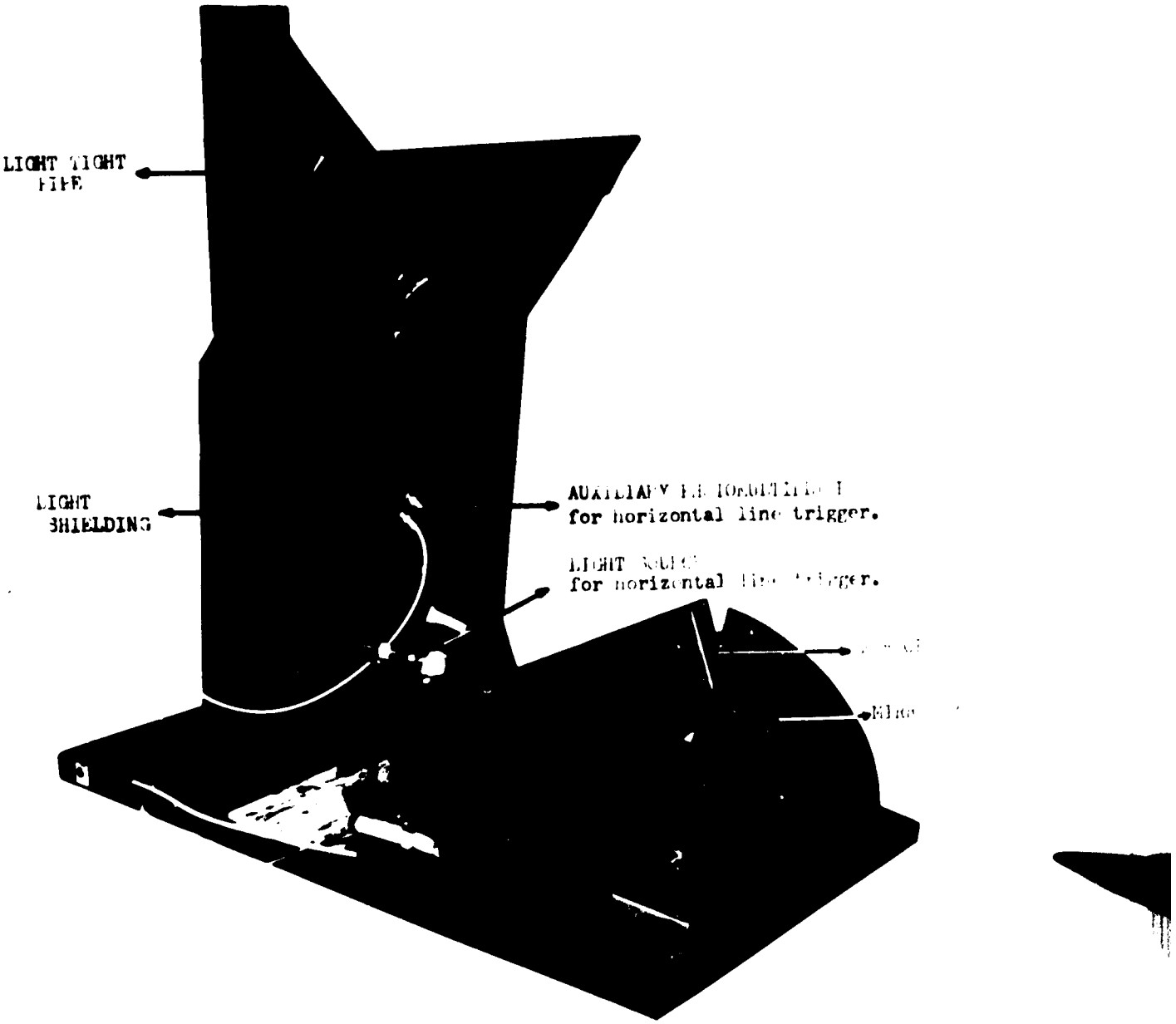

FIG 4: PHOTOGRAPH OF MECHANICAL SCANNER

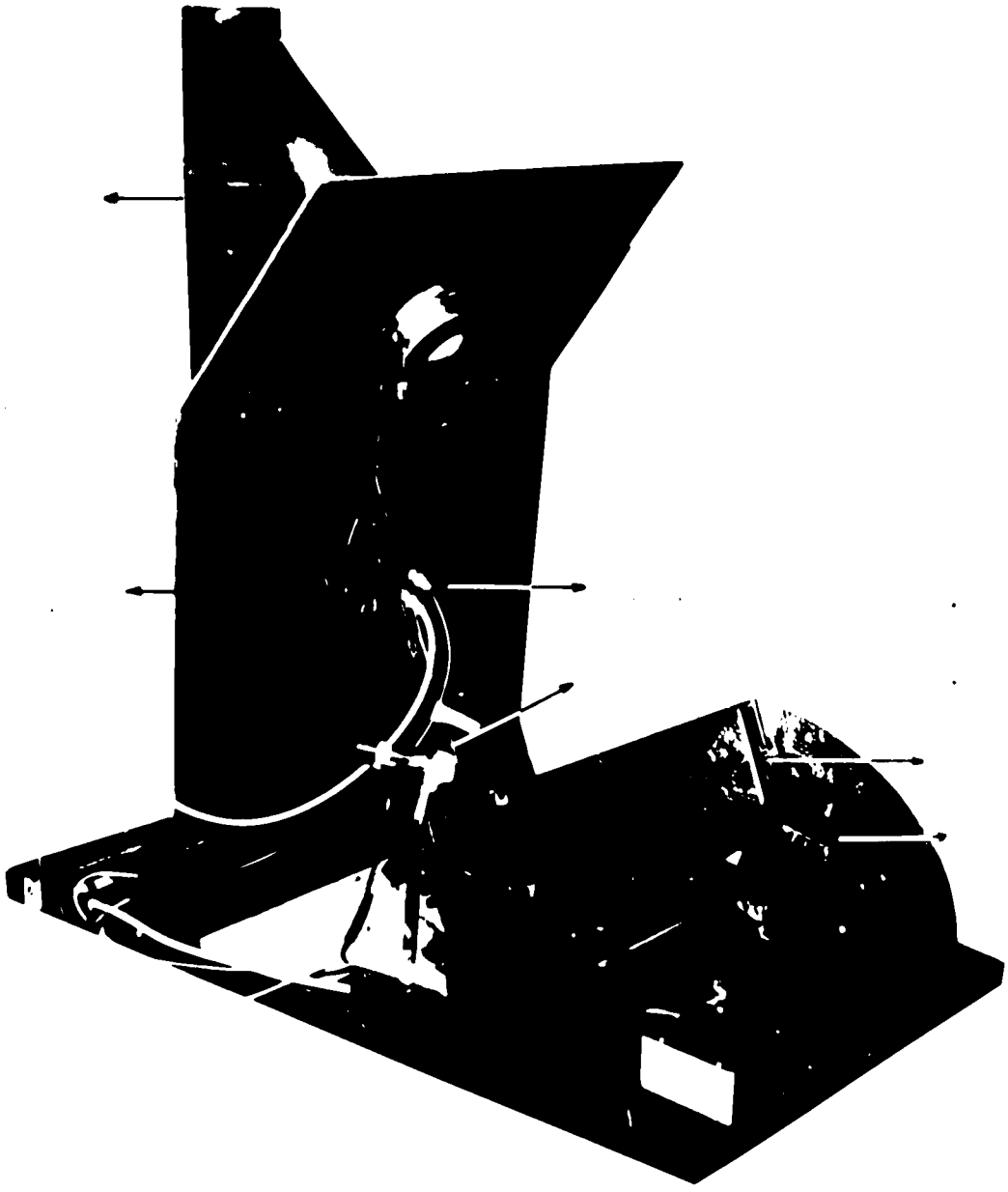

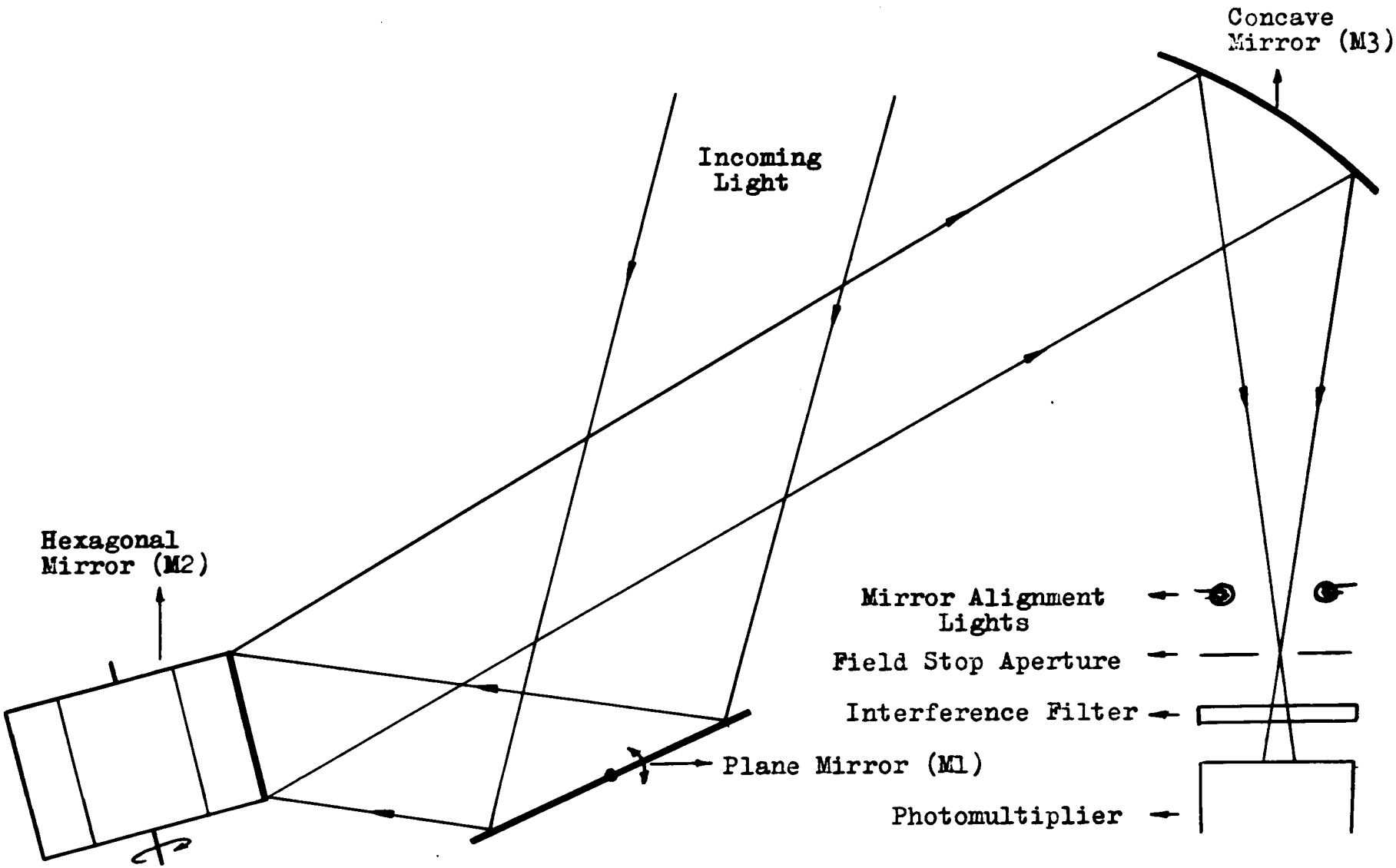

Fig. 5: Optical Arrangement of the Scanner

CHAPTER 3

MECHANICAL SCANNING PHOTOMETER

In this chapter, the optical design, the mechanical design, the engineering problems involved in the construction of the scanner, and also the electronics involved in the reproduction of a picture from the scanner information will be described. Finally, the laboratory tests performed on the scanner will be discussed.

A photograph of the scanner is shown in Fig. 4.

(i) Optical Design

Light from an area in the sky A (Fig. 5) is reflected from the plain mirror 1, onto one face of the hexagonal mirror 2, and onto the concave mirror 3. Mirror 3 focusses the light onto a field stop aperture, then to the photocathode of a photomultiplier.

First, consider mirror 2 held stationary as mirror 1 oscillates backwards and forwards about an axis perpendicular

to the plane of the page. The light that falls onto the photomultiplier now originates from a line in the sky, which is in the plane of the paper.

If mirror 1 is now held stationary while mirror 2 rotates about its near-vertical axis, the light that enters the photomultiplier comes from a line in the sky, perpendicular to the plane of the paper.

Thus, if mirror 1 oscillates slowly and mirror 2 rotates rapidly, the system scans out a rectangular area of the sky, mirror 1 providing the vertical sweep and mirror 2 the horizontal sweep. Mirror 1 oscillates through 60 degrees and, by suitable positioning of mirror 2, the system scans over an area of the sky equivalent to an angular field of 120 x 120 degrees.

The aperture placed on top of the photocathode defines the angular resolution of the scanner. This is given by the ratio of the aperture diameter to focal length of the concave mirror, and is set at 1.2^{o} (aperture diameter

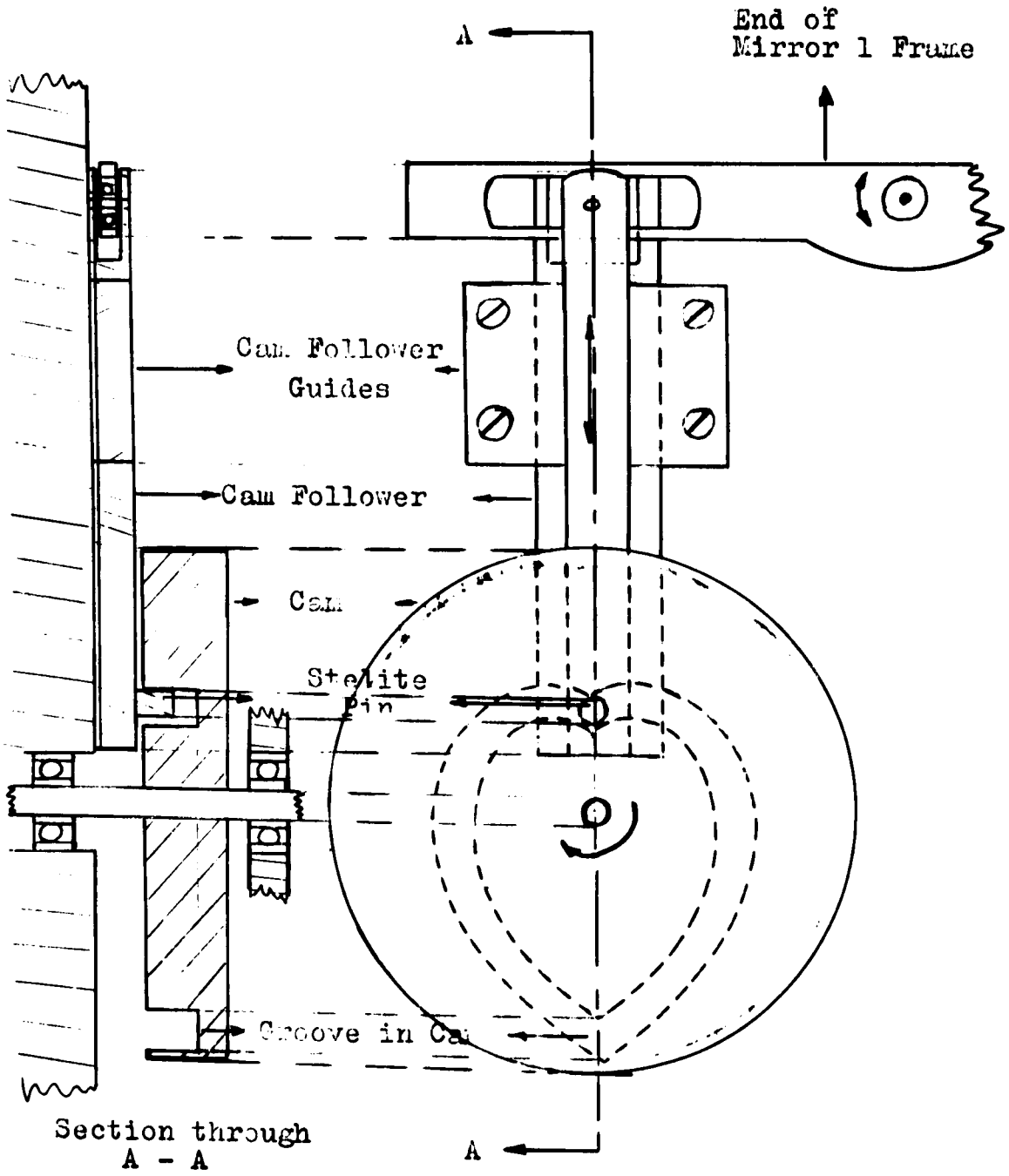

Fig. 6: Cam System for Mirror No. 1 Drive.

is 1.02 cm, and focal length of mirror 3 is 50 cm). Auroral light passing through the field stop converges at an angle of about 5 degrees which is sufficient to stay within the bandpass of an interference filter placed on top of the photocathode.

Mirror 2 forms the entrance pupil stop. Mirrors 1 and 3 are made sufficiently large so that this is the case for light incident from all directions within the scanner field of view.

(ii) Mechanical Design

Mirror 1 consists of a plane mirror 5" x 20" which oscillates with constant angular velocity about its long center axis. This motion is accomplished by means of a cardioid-shaped, push-pull cam (Fig. 6). The oscillatory motion is transferred from the cam to the mirror by means of a cam-follower. One end of the cam-follower is attached to a slot in the mirror frame, the other end follows the cam through a solid, stelite pin, which is rigidly attached to the

cam-follower, and runs in the cam. Because of the nearly instantaneous reversals in the mirror's angular velocity, the push-pull cam (rather than a push cam with a spring return), and the solid stelite pin (rather than steel pin and a brass roller) were found to be essential.

Mirror 2 consists of a hexagonal aluminum prism with front coated mirrors, each 2" x 2", glued to its six sides. The resulting mirror withstands the vibrations and forces produced by rotating the mirror at speeds up to 10,000 rpm.

Mirror 3 is a 3" diameter, 21" focal length, concave telescope mirror.

(iii) Electronics and Reproduction of the Picture

The picture of the sky, displayed on an oscilloscope screen, is built up of about 100 horizontal lines, each corresponding to a horizontal line in the sky and each line in the sky differing in elevation angle by about 1.2

degrees (equal to the designed angular resolution).

The horizontal sweep is provided by the oscilloscope horizontal sweep, synchronised to the scanner by means of the vernier sweep speed adjustment on the scope. The sweep is triggered by a pulse provided by the scanner. A small light-source produces a narrow beam of light, which is reflected off mirror 2 into an auxiliary photomultiplier tube, at the beginning of each horizontal scan. A blue filter is placed in front of the light source to prevent scattered light passing through the green interference filter and appearing in the final picture.

The slow vertical sweep signal is generated by the scanner as a voltage, always proportional to the orientation of mirror 1. No completely satisfactory method has as yet been found to generate this voltage. A linear carbon or wire-wound potentiometer used as a potential divider is found to be electrically noisy due to changes in contact resistance. They also deteriorate rapidly.

An R.C. circuit, which charges as the mirror rocks in one direction and discharges as the mirror rocks in the opposite direction, gives a clean, straight-sectioned triangular trace, but the state of charge is not at all times proportional to the position of the mirror and so does not immediately adjust to changes in the mirror's angular velocity.

An optical method appeared to be an improvement over the above methods. A blade attached to the mirror shaft varied the amount of light incident on a detector as the mirror moved to and fro. A photoresistor used as the detector was found to be adequate at low scanning rates, 1 or 2 scans per second, but due to the time response of the cell (about 10 mS), it was inadequate at fast scan rates. This time lag caused images to be displaced vertically on the oscilloscope screen on consecutive scans. This effect could be overcome by photographing individual pictures or every other picture.

A phototube, with microsecond response, was used

in place of the photoresistor. This was found to be unsuitable. The tube had an extremely high input impedance and so picked up electrical noise given off by the electric motors.

It is hoped that a special application potentiometer will solve this problem. The potentiometer has low contact resistance noise level and an extremely long life.

The detector used to detect the auroral light is an EMI 9514S photomultiplier. This tube is particularly suited for this purpose due to its high gain and very low dark current (see Chapter 2).

The electronics was originally designed so that the photomultiplier current varied the intensity of the beam on the oscilloscope screen. This was achieved by amplifying the photomultiplier signal in a D.C. amplifier and using the output of the amplifier to intensity modulate the oscilloscope beam.

Because of the difficulty in producing stable high

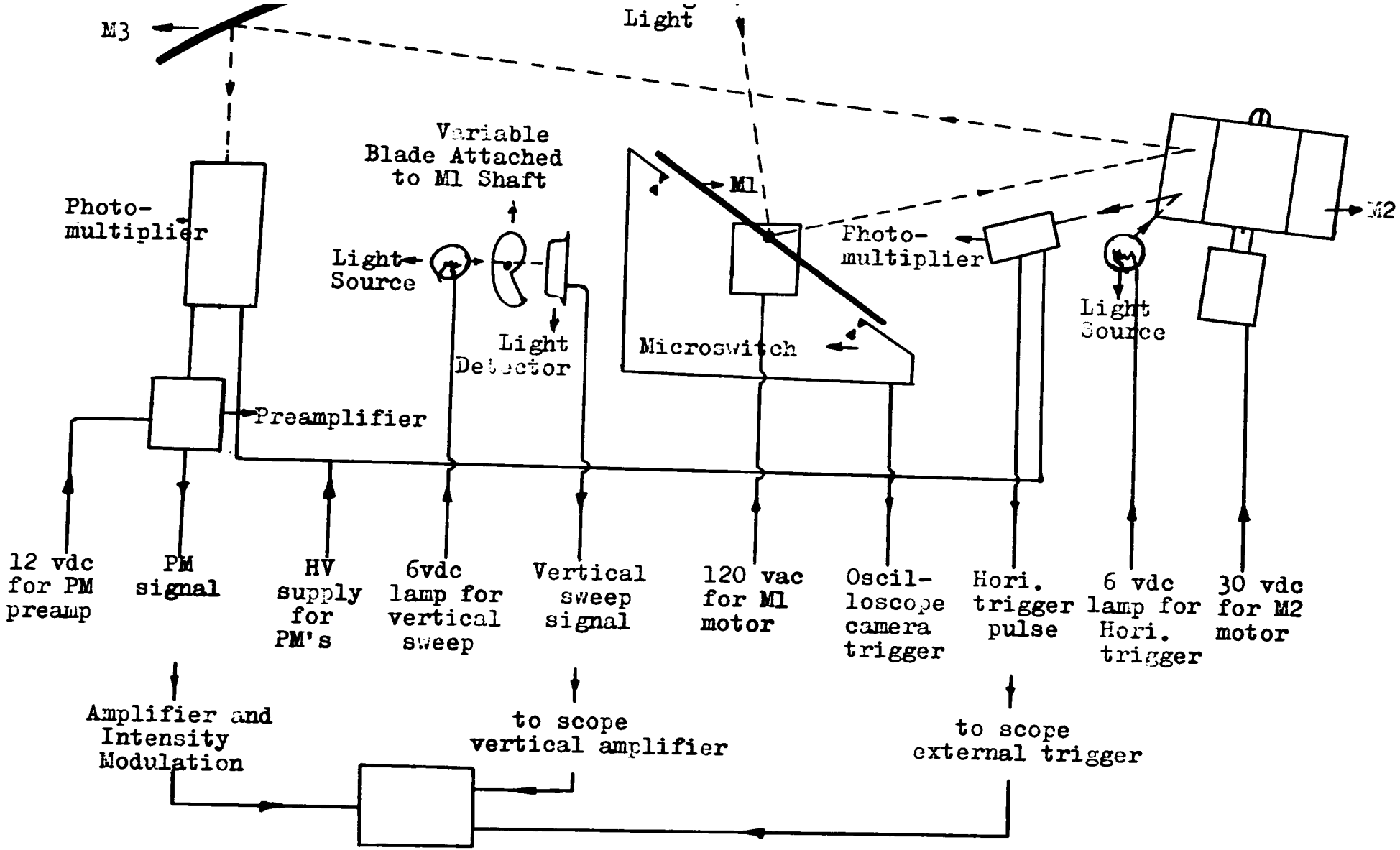

Fig. 7: Electrical Arrangement of the Scanner.

gain D.C. amplifiers and also since the signal for faint aurora was in the form of isolated photoelectron pulses, the electronics has subsequently been changed to extremely fast pulse circuitry, with an electronic time constant of about 0.1 μS. Unfortunately, the amplifier gain was still insufficient for single photoelectron pulses to produce a spot of recordable intensity on the oscilloscope (see Chap. 2(ii)a).

With this system a bright aurora will produce a large number of single pulses all of equal brightness on the oscilloscope screen and a faint aurora, which produces only single or double photoelectron pulses, should now produce a recordable image.

Fig. 7 shows a schematic diagram of the scanner with the various signals and power requirements indicated.

(iv) Operation

The picture displayed on the oscilloscope screen, and a clock alongside, are photographed using a 16 mm Bolex

movie camera. The camera shutter is held open whilst the picture is built up on the screen. The film can be advanced either at the end of each consecutive scan or at the end of each cycle (thus recording up and down scans). This operation is triggered by microswitches depressed by mirror 1 at each extreme of its motion, which corresponds to the completion of a scan. The film camera is operated by an external solenoid.

The whole system is self-synchronised. Any changes in the speed of mirror 1 do not necessitate adjustments, except possibly for incorrect exposure in the filming process; however, even here there is a certain amount of latitude. Small variations (about 10%) in the rotation speed of mirror 2 causes the picture to expand or compress horizontally. This necessitates no adjustments unless the mirror speed increases by such an extent that the time, between the horizontal line trigger pulses from the scanner, is less than the time required for the oscilloscope to sweep out a horizontal line. In this case every other trigger pulse will trigger

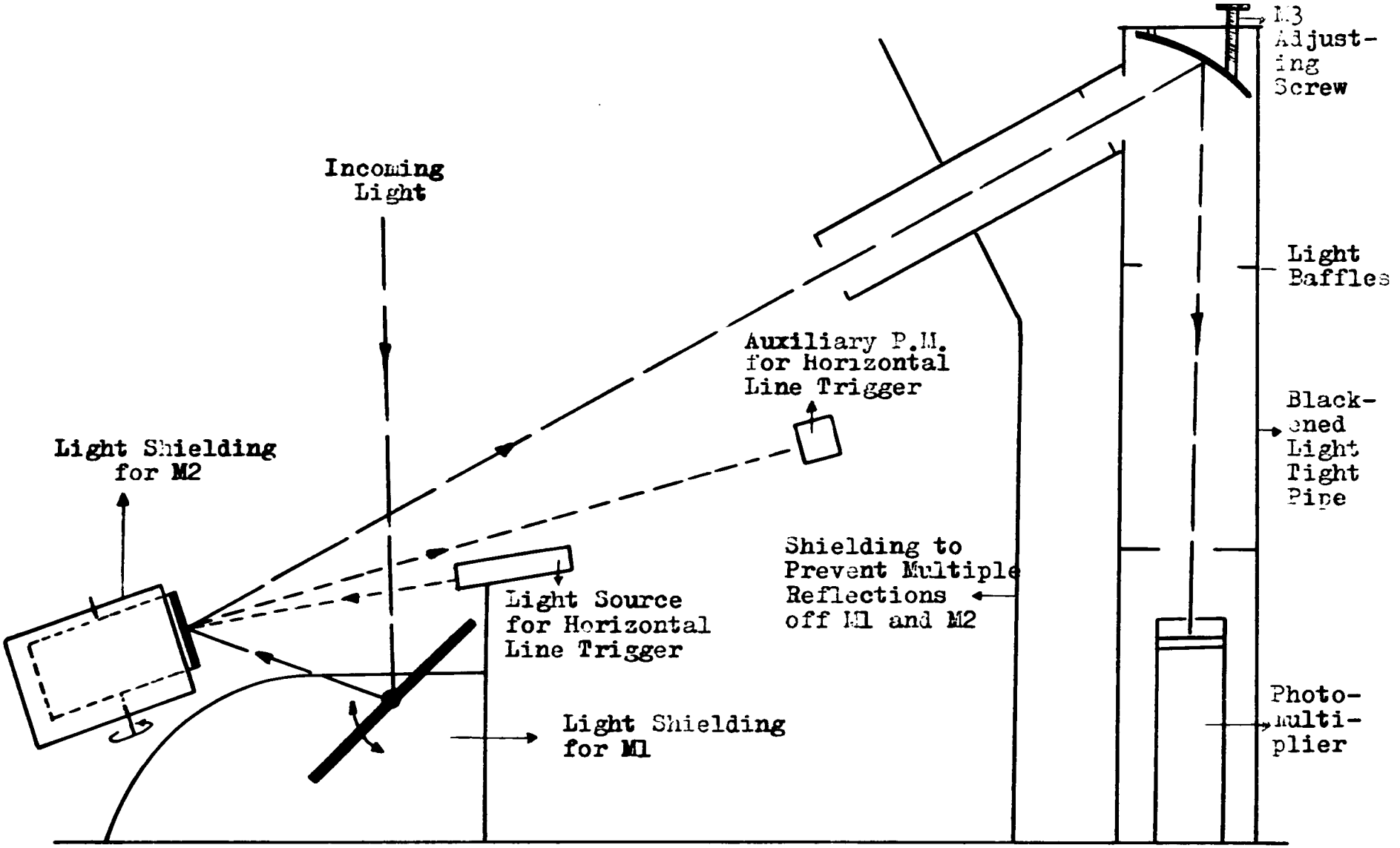

Fig. 8: Details of Scanner Light Shielding

the oscilloscope and the number of lines per picture will be reduced by a factor of two.

(v) Laboratory Testing

The mirrors were aligned in the following manner: Lights were permanently built into the scanner on either side of the field stop aperture. Mirror 3 was adjusted so that the lights could be seen via mirrors 1, 2, and 3 from all possible positions within the scanner field of view.

Scattered light problems have been overcome by suitable screening and by enclosing mirror 3 and the photo-multiplier in a blackened light-tight tube containing several apertures and baffles. It was found that extraneous light from a region outside that scanned was entering the photo-multiplier by multiple reflections from the two mirrors (Fig. 8). This has been eliminated by fixing a blackened screen in such a position as to completely cut out the light from the offending region.

Side screens were placed at both ends of mirror 1 to prevent light entering the photomultiplier housing, from a single reflection off mirror 2.

The reflectivity of the scanner mirrors was found by taking the ratio of the photomultiplier output when viewing a standard source first through all three mirrors, then directly.

The Low Brightness Source (L.B.S.) consisted of a light bulb, operating under controlled conditions, situated behind two sheets of opal glass to produce a uniformly illuminated surface. The brightness of the surface could be varied by placing neutral density filters in front of the light source. The source was calibrated by Defence Research Northern Laboratory at Fort Churchill, to read in Kilo Rayleighs per Angstrom bandwidth of the detector at a particular wavelength.

The source was placed in front of the scanner, sufficiently close that it presented a solid angle much

larger than that viewed by the scanner, and the mirrors adjusted to obtain the maximum output from the photomultiplier as measured on a D.C. voltmeter. Part of the illuminated screen on the source was then masked off to leave an area of 2" x 2" equivalent to the area of mirror 2. The source was then placed between mirror 2 and mirror 3 pointing towards mirror 3 and the photomultiplier output again noted.

The ratio of the former to the latter of these two readings gives the reflectivity of mirror 1 and mirror 2 and was found to be 25%. That is, the average reflectivity of each mirror was 50%. The reflectivities of the mirror faces of mirror 2 were found to differ from one another by 20% due to variations in the aluminising.

The scanner was found to give a different signal strength for the source, when placed in different positions within the field of view of the scanner. This was attributed to the change in receiving area of mirror 2 due to light

falling onto it obliquely.

The angular resolution was checked by measuring the width of the spot produced on the display system, by a point source at a large distance from the scanner. The horizontal resolution was found to be 1.3 degrees.

The sensitivity of the scanner was measured in the laboratory, and found to be numerically similar to that calculated for the particular operating conditions. This was done by finding the fastest scanning speed at which the scanner gave a continuous image of the calibrated L.B.S. This operating condition correspondedto a known number of photoelectrons per picture element, which could be related to the brightness of the L.B.S.

(vi) Interpretation of Scanner Photographs

The scanner was designed to have a field of view of 120° by 120°. At high scanning rates the field was reduced to 90° in the horizontal scan due to a time lag in the oscilloscope between the end of one line and the reset for

Fig. 9: Example of Scanner Photograph

Fig. 9: Example of Scanner Photograph

the beginning of the next line. This lag amounted to about one-third of the total horizontal scan time. A typical scanner photograph is shown in Fig. 9. The dark region on the top edge of the photographs, just right of center, was produced by the screening introduced to prevent scattered light from entering the system. The small dark region on the lower edge of the photograph is caused by the housing for mirror 2 and serves to define the direction the scanner is pointing in the photograph.

It is useful to consider the scanner display corresponding to a grid of parallel lines of constant latitude and longitude situated at an altitude of 100 km. (The lines have been considered 60 km apart.)

To an observer on the surface of the earth, the lines of longitude would appear parallel overhead and converge in the north and south. These lines would also appear to crowd together in the east and west. The lines of latitude would appear similar.

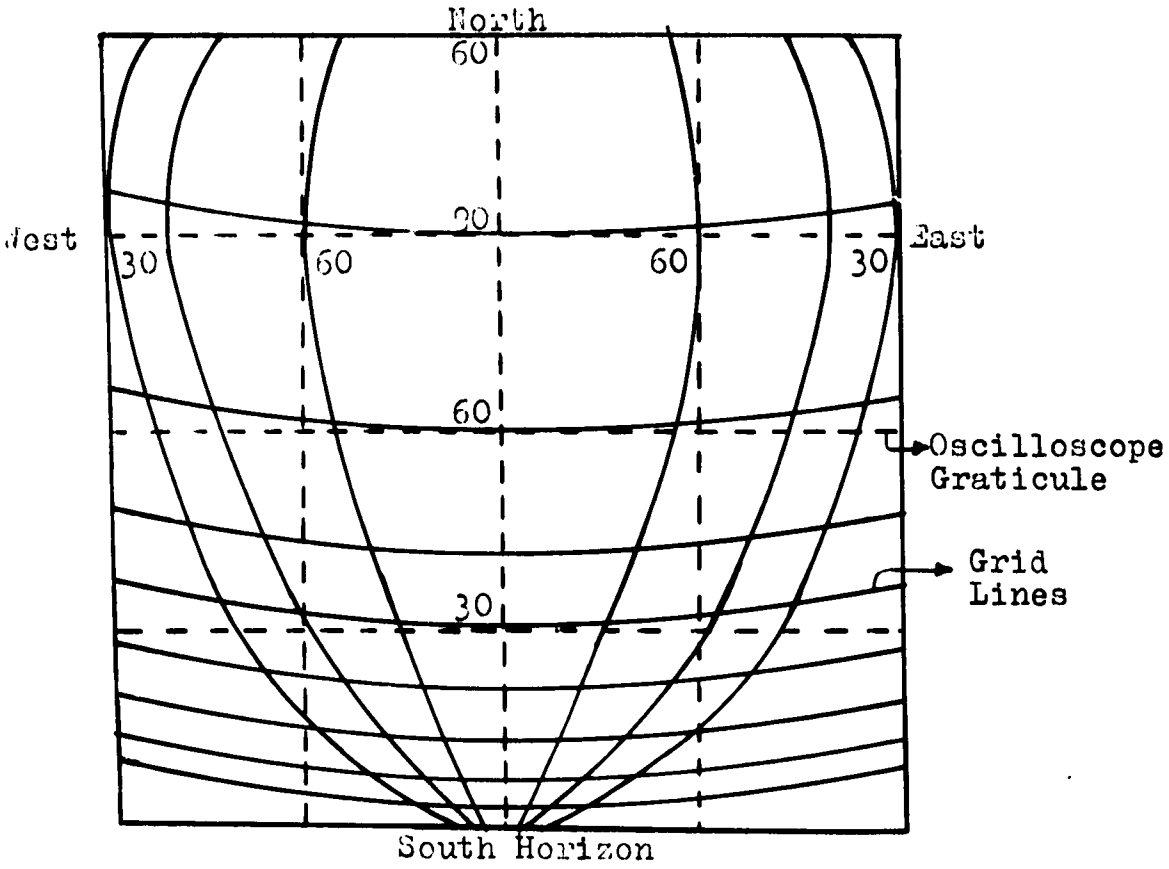

Fig. 10: Rectangular Grid as Displayed by Scanner.

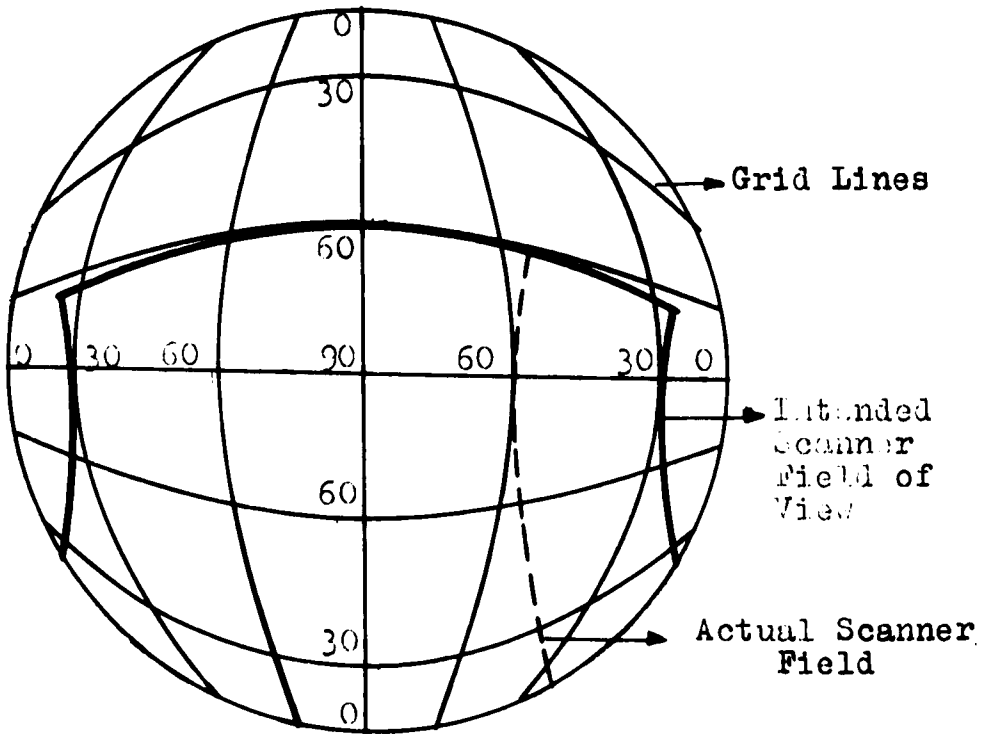

Fig. 11: Rectangular Grid as Displayed by All Sky Camera.

The scanner, if it were pointing south, would display the grid approximately as shown in Fig. 10. The lines of longitude would appear parallel overhead and converge in the north and south. These lines would also appear to crowd together in the east and west. The lines of latitude would appear parallel but slightly curved (the latter due to the fact that mirror 2 does not rotate about a vertical axis). These lines would appear to crowd together in the south. Thus, the scanner display is very similar to that seen by the observer.

An All Sky Camera would display the grid as shown in Fig. 11. The designed scanner field and the actual scanner field of view are shown.

CHAPTER 4

RESULTS OBTAINED WITH THE SCANNING AURORAL PHOTOMETER

The scanner was first used in Fort Churchill, Manitoba, to take moving photographs of visible aurora. After initial problems of unreliability, due to extremely cold conditions, had been overcome, the scanner ran continuously at about 3 scans per second for 3 nights.

As well as the scanner photographs of the aurora, a verbal, tape-recorded description of the aurora was made during the major events, mainly to facilitate recognition of the various auroral features in the scanner photographs. All Sky Camera (A.S.C.) photographs were also available for comparison.

During the night of April 21st to 22nd, the scanner was in operation at the same time as a balloon experiment involving auroral x-ray detecting equipment. For details of this apparatus see Appendix.

Fig. 12: Photograph of Twilight Aurora

The A.S.C. film indicated seven occasions during the night of April 21st to 22nd, on which visible aurora was present. On the first two of these occasions the scanner was not operating, and in one other event the aurora occurred in the region of the sky not covered by the scanner. The remaining four auroral events were detected by the scanner.

The scanner also detected visible aurora during twilight (Fig. 12). This could not be seen with the naked eye or on the A.S.C. film, but could just be seen by looking through a narrow band interference filter after the eyes had become adapted to the dark. The scanner photograph suggests the auroral intensity was probably between I and II.

X-rays were observed on all four occasions on which the scanner detected visible aurora.

During the major auroral display of the evening (the event analysed in this chapter), the scanner ran at about 50 scans per minute, corresponding to an exposure of 1.2 seconds per picture. During this display the oscillo-

scope camera, recording the auroral pictures produced by the scanner, was operated by hand due to a malfunction in the electronic circuit which operated the camera. Shortly after the event, the malfunction was rectified and the scanner ran unaided for the rest of the night. Unfortunately, no other large auroral displays occurred.

Fort Churchill is situated at a latitude of $58^{\circ}45'$ and longitude 94°, just north of the auroral zone, which is between 65° and 70° geomagnetic latitude or 57° geographical latitude at 94° longitude.

In all the scanner photographs the scanner was directed south $25^{\circ} \pm 5^{\circ}$ east, so that the balloon appeared in the center of the picture during the period of interest.

The position of the balloon, from radar data, was given as S 24° E, elevation 33°. The aurora at the 100 km height above the balloon is at an elevation of 66° on the photographs, i.e., halfway up the photographs, and situated directly above the dark region on the lower edge of the

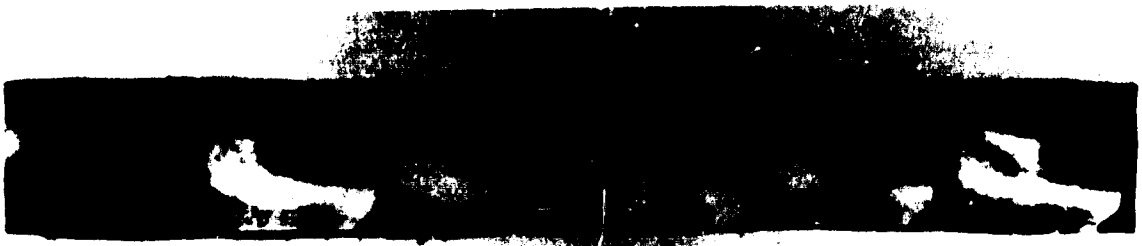

A.S.C. Photograph.

0051:10.

Now faded out.

0051:20.

Brightening again.

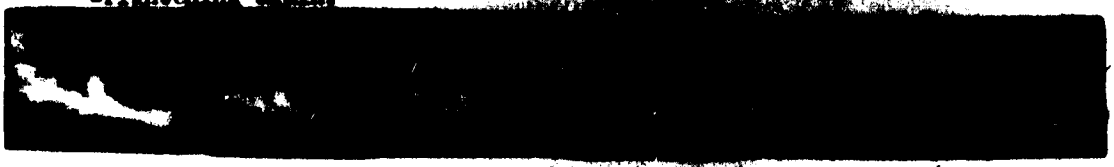

Bright corona overhead.

0051:30.

Brightening in east.

Type B in east.

0051:40.

Motions and draperies overhead and to west.

0051:50.

Now more spread out, band not

0052:00

A.S.C. Photograph.

FIG 13: ONE MINUTE SEQUENCE OF

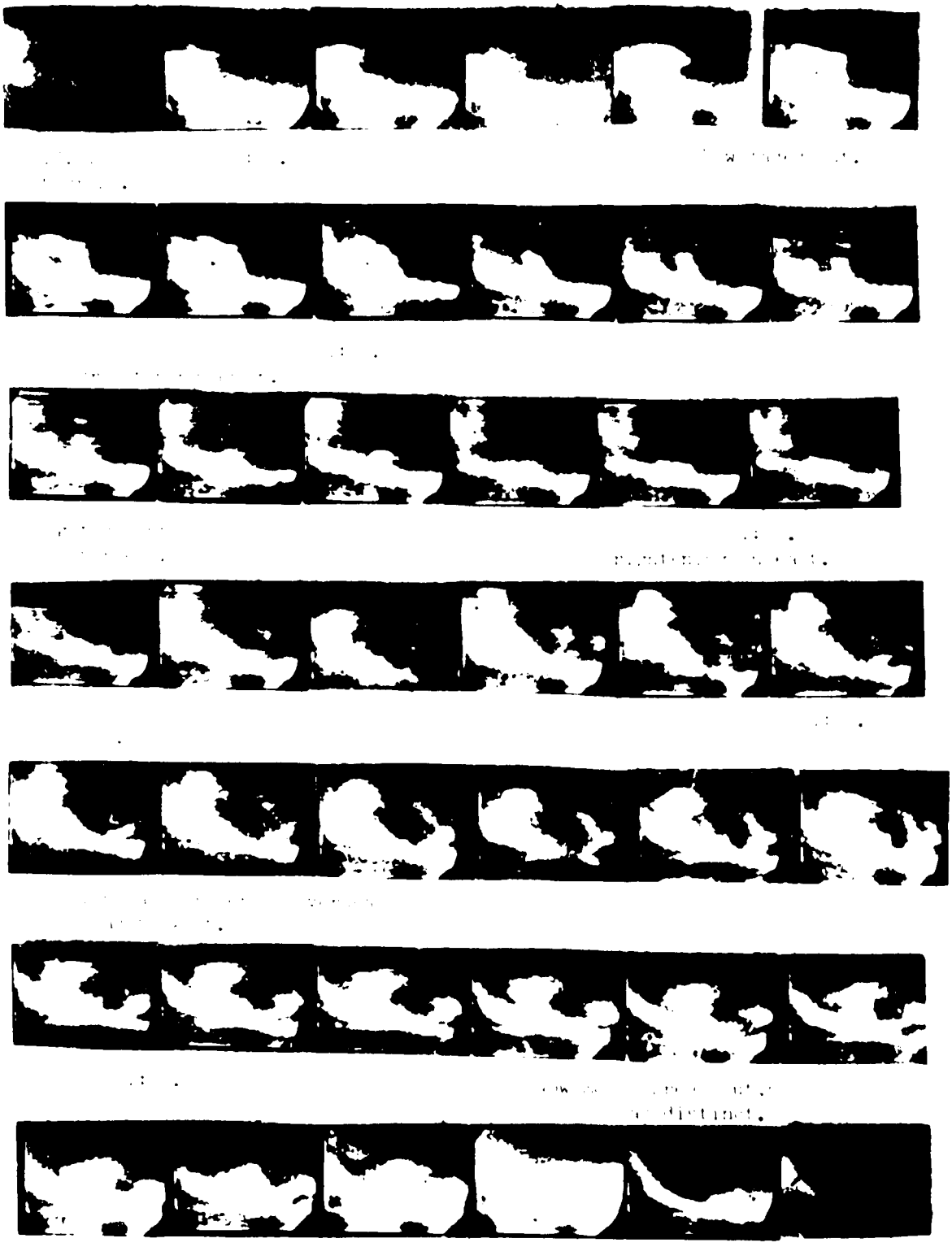

photographs.

All times in the following analysis are Central Standard Time (CST.).

(i) Examples of Auroral Photographs Obtained With the Auroral Scanner

Fig. 13 shows a block of one minute of scanner data. Below each photograph is the time in CST, and a tape recorded description of the aurora made by an experienced observer. The two ASC photographs, corresponding to the beginning and the end of this sequence are shown. The scanner incorporated a 5577 $\mathring{A}$ (14 $\mathring{A}$ half-width) interference filter. The photographs show a bright band stretching from west to east on the southern horizon. In the first photograph a split is observed in the west end of the band.

At 0051:10 the split has widened, and by 0051:15 the upper part has developed into another band which can be seen separated from the main lower band.

This new band moves rapidly across the sky and by 0051:30 has completely disappeared into the south (estimated velocity, 7 km/sec). At 0051:25 the west end of the band has again brightened and split and by 0051:40 another bright band of aurora can be seen moving from the west to the south at an estimated speed of about 7 km/sec. At 0051:50 the band from the west can be seen drifting rapidly towards the band in the south. In the last photograph at 0052:00 most of the auroral activity has disappeared.

The photographs have an exposure of about 1.3 seconds each. Next-to-the-last photograph has an exposure of about 3 or 4 seconds.

It is obvious that the verbal description of the aurora does not fit the scanner photographs too well. Assuming that the timing is correct in both cases, the most likely reason for this is that the observer was not looking at the same area of the sky as the scanner. Also, due to the extremely rapid movements of the aurora, it was impossible for

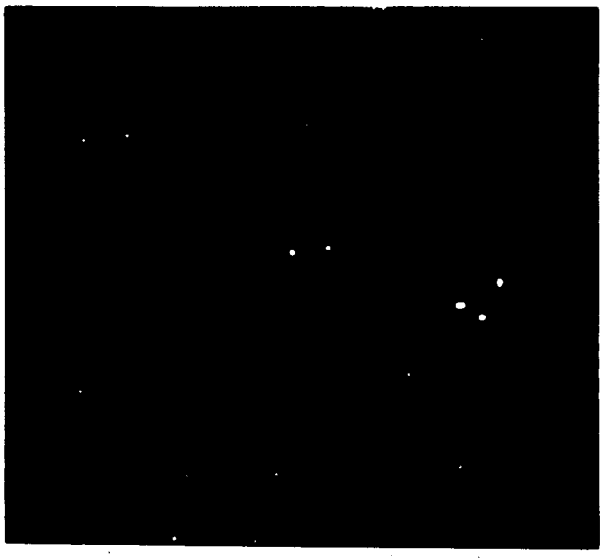

Fig. 14(a): Example of Faint Aurora

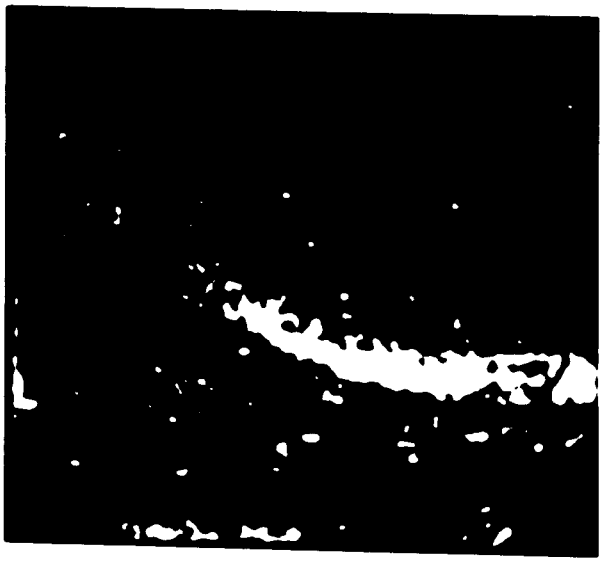

Fig. 14(b): Example of Faint Aurora Taken with Time Exposure

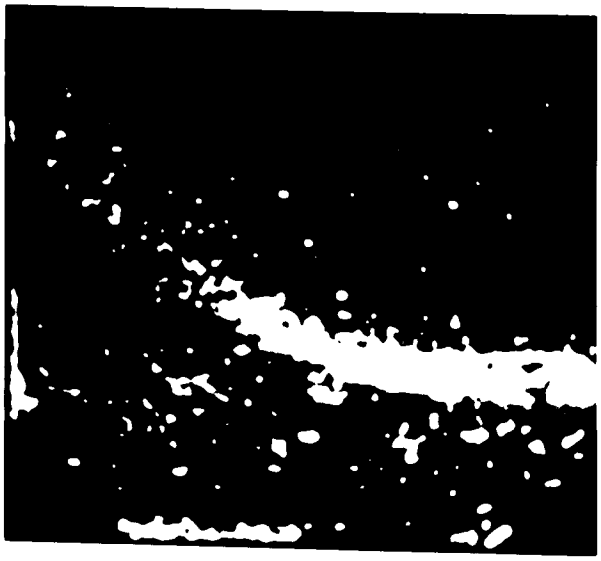

the observer to describe all the activity. It is apparent from these pictures, that it is very difficult to provide an adequate verbal description of an active aurora even with the aid of a tape recorder. During periods of less active aurora, the recorded description fits the gross features of the aurora seen in the photographs quite well.

Most of the photographs in Fig. 13 are examples of very bright aurora, which caused saturation of the oscilloscope phosphor. Brighter aurora than this would not appear brighter on the screen.

Fig. 14(a) shows an example of faint aurora--a band that occurred at 0222:00 on the night of April 21st to 22nd. This band of intensity I was invisible to the naked eye due to a bright moon.

Fig. 14(b) shows the same band photographed with a longer exposure time (about 3 seconds compared to 1/2 second for Fig. 14(a)). This was obtained by holding the oscilloscope camera shutter open for several scans.

The band at 0222:00 shows a number of spots of light accumulating in the region of the band. The odd spots on the remainder of the screen are caused by the larger photomultiplier dark current pulses, and possibly airglow.

(ii) Qualitative Correlation Between Visible Aurora and X-rays

The auroral activity between 0048:00 and 0100:00 CST. (night of April 21st and 22nd, 1964) can be divided into two parts: 0050:00 to 0052:30, and 0052:30 to 0056:00. The scanner photographs show bright aurora between these times separated by a distinct quiet period. The x-ray count rate also shows two distinct periods of activity. The Fort Churchill magnetometer and riometer records give insufficient time resolution to permit the use of this data in the analysis.

A detailed correlation between the visible aurora and auroral x-rays has been attempted, the significance of which is substantially reduced for several reasons.

1. The resolving time of the x-ray data was

inadequate to enable using all the scanner photographs. As described in the Appendix, the x-ray data, for x-ray energies between about 15 and 100 KeV, was processed in a pulse-height analyser and displayed every second on an oscilloscope in the form of a histogram. The histograms were photographed. After eight seconds accumulation the analyser channels were reset to zero. Unfortunately, due to several faults and the low count rates, only the eight-second total counts were considered sufficiently reliable. The following analyses are qualitative and thus, up to a point, independent of these faults. The counts shown on the graph (Figs. 15, 16 and 17) correspond to four seconds on either side of the time shown.

2. The exact timing of the scanner photographs was unobtainable from the data. The second dial on the clock, photographed alongside the auroral pictures, could not be read. Thus, the pictures could only be timed accurately at the instant the minute dial changed. These times are accurate to ± 1 second and intermediate times, obtained

by interpolation, have a possible error ±5 seconds.

3. The field of view of the scanner was inadequate. Although the balloon was almost in the center of the scanner photographs, on three occasions it appears as though the x-rays can only be associated with aurora outside the scanner's field of view. The region of the sky overhead, blanked out by screening (see Chapter 3) and the right-hand edge of the photographs, represents a horizontal distance of about 60 km from the 100 km altitude point above the balloon (balloon zenith). It has been found that x-rays originating from distances of up to 100 km can produce detectable increases in a balloon detector (N. R. Parsons, private communication).

The following analysis was carried out by noting changes in the x-ray count rate and then the changes in the visible aurora for the corresponding time.

Figs. 15, 16 and 17 show the x-ray count rate per second, averaged over an eight-second period, for the times

0049:30 to 0052:30 CST	Fig. 15
0052:30 to 0054:00 CST	Fig. 16
0054:00 to 0057:00 CST	Fig. 17.

Only the x-ray energy channels 2, 3, 4, 5 and 7 are shown. The counts in channel 6 overfilled the analyser channel for most of this period as more than 250 x-rays of this particular energy were detected during the eight-second accumulation interval.

For each variation of the x-ray count rate a series of scanner photographs are shown. Times are indicated alongside the photographs.

At about 0049:00 a bright band could be seen in the south; at 0050:00 the band split into two and continued to brighten. Unfortunately, for most of this period the scanner film was fogged. Also, the timing of the photographs could only be determined to within $\pm$10 seconds, as only one reference time was obtainable. However, it is obvious that the auroral intensity steadily increased. This corresponded to the increase in the x-rays during this period.

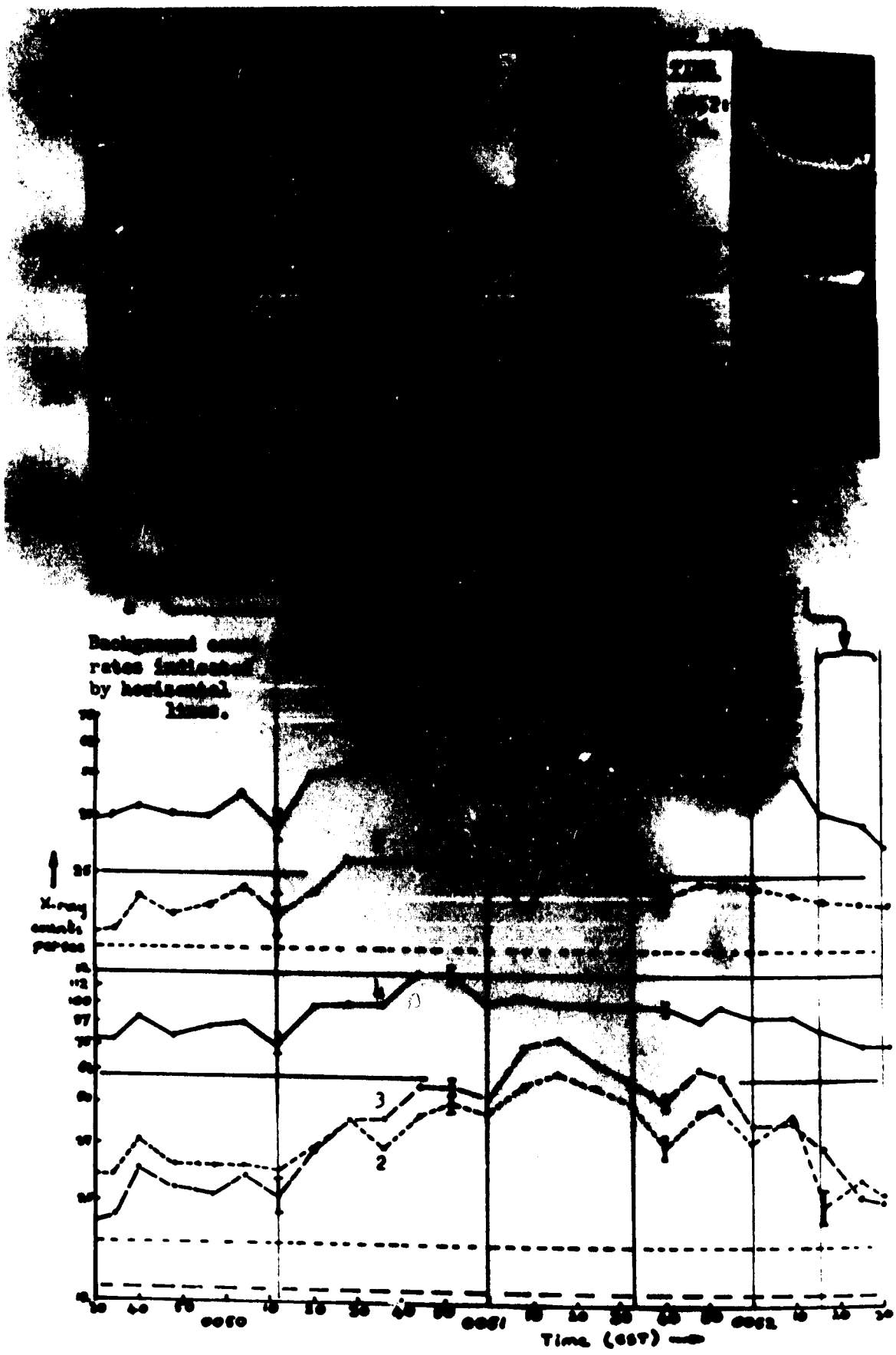
Background
rates indicated
by horizontal
lines.
X-ray
counts/
minute
3
2
0000
0001
0002
Time (GST)

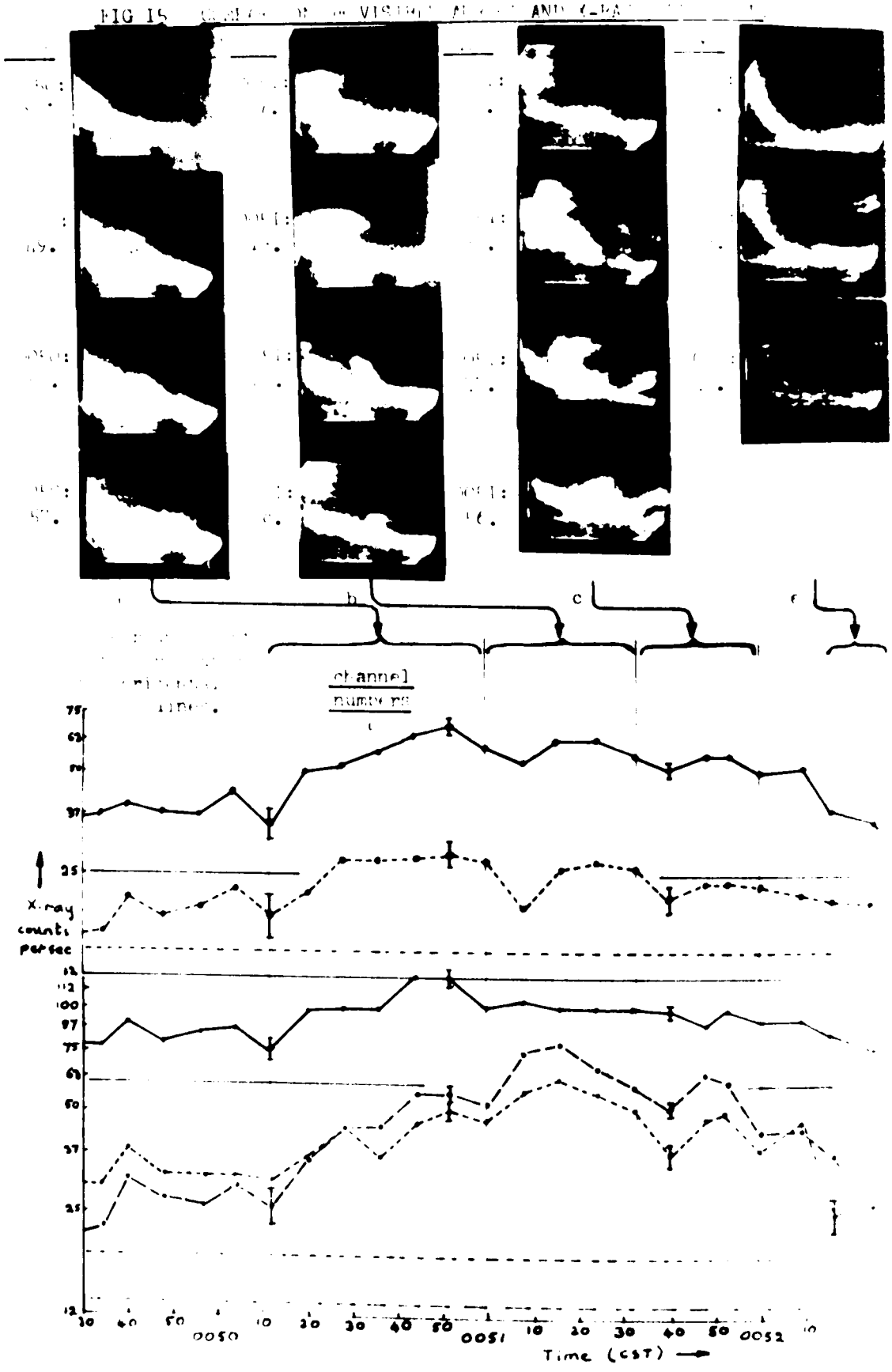
b
c
channel
number
X-ray
counts
per sec
0050
0051
0052
Time (CST)

No sudden increase can be seen in the aurora at 0049:40, corresponding to the sudden increase in the x-rays at this time.

The most interesting and significant feature of the breakup period between 0048:00 and 0052:30 was the appearance of three distinct auroral events, designated (a), (b) and (c) in Fig. 5.

Event (a): At 0050:00 the band on the southern horizon split into two horizontal bands. At 0050:40 the upper part of the band developed a fold, which moved from the west to the south, at 1.4 (±50%) km/sec, to about 40 km from the balloon zenith. (This was described as S form and Type B red by an observer.)

('Type B red' aurora is the name given to the bright mauve-red lower border seen during a very active auroral breakup. It occurs at a much lower altitude than normal arcs and bands and arises from molecular nitrogen and ionised molecular oxygen emissions. The electrons producing this type

of aurora are more energetic than those producing the higher altitude aurora, and so are more capable of producing x-rays at balloon altitudes).

This intensification in the optical aurora, corresponded to a maximum in all x-ray channels at 0050:45. The low energy channels 2, 3, 4 and 5 showed increases of more than six times the probable error. Channel 7 increased by only three times the error. The increases are given relative to the counting rate at 0050:12, the time corresponding to the beginning of this event.

The four photographs show the double band, from which the fold developed, and the progression of the fold from west to south.

Event (b): A second disturbance started at 0050:56 as a band in the west (band showed Type B red colour--visual report). The band moved rapidly, at about 7 km/sec, across the sky to the south, drifting towards the band in the south and disappearing at 0051:33. Fig. 12 shows the entire sequence of

pictures for this event. The main features of the event are shown in Fig. 15(b).

Maxima in the x-ray counting rates occurred at 0051:15, the increase starting at 0051:00 for channels 2, 3 and 4 and 0051:08 for channels 5 and 7. The increases amounted to more than three times the probable error for all channels except 4. Channel 4 showed no increase.

It is noted that the low energy channels 2, 3 and 4 show a minimum at 0051:00 and channels 5 and 7 at 0051:08. This suggests that event (a) was connected with a higher energy x-ray flux than event (b). Between 0051:00 and 0051:08 the build-up of low energy x-rays due to event (b) was greater than the decrease of x-rays of this energy following event (a). Thus, the low energy x-ray count rate increased. At high energies the rate of increase of x-rays due to (b) was less than the decrease following (a), and so these x-rays decreased. In channel 4 the counts stayed constant; the increase due to (b) was equal to the decrease

of x-rays from (a). This is borne out by energy spectrum curves (see next part of this chapter).

Event (c): While event (b) was still in progress, a third event, (c), began. The third event was very similar to event (b). It first appeared as a band in the west at 0051:27. At 0051:35 the band brightened appreciably within 2 or 3 seconds then moved from the west to the southeast, at 7 (±50%) km/sec, passing over the balloon at 0051:50. By 0052:00 the band had drifted far into the south. The minimum between events (b) and (c) occurred at the same time for channels 2, 3, 5 and 7. The x-ray maxima occurred at 0051:48. Channels 2 and 3 increased by about four times the error. Channel 4 showed no change. Channels 5 and 7 increased by an amount approximately equal to the probable error in both cases. The whole sequence of photographs corresponding to this event is shown in Fig. 13. The main features are shown in Fig. 15(c).

Event (d): The band described in event (c) could be seen moving southeast until 0052:30, by which time it was estimated to be in excess of 200 km from the balloon zenith. From 0052:00 to 0052:30 the x-ray count rate steadily decreased, coinciding with the southward drift of this band. At 0052:30 all the x-ray channels showed count rates of little more than the estimated background due to cosmic ray x-rays.

Event (e): A bright band appeared in the east 100 km from the balloon zenith between times 0052:26 and 0052:40. Only channel 2 showed an increase at this time; the other channels decreased steadily. The increase amounted to about 20% (or $1\frac{1}{2}$ times the probable counting rate error). This event is shown in Fig. 15(e). The band appeared to drift from the eastern region of the sky to overhead, then drift back into the east.

The band appears as a double structure in the photographs. This structure is apparent in several photographs. It could be attributed to an instrumental fault, but as

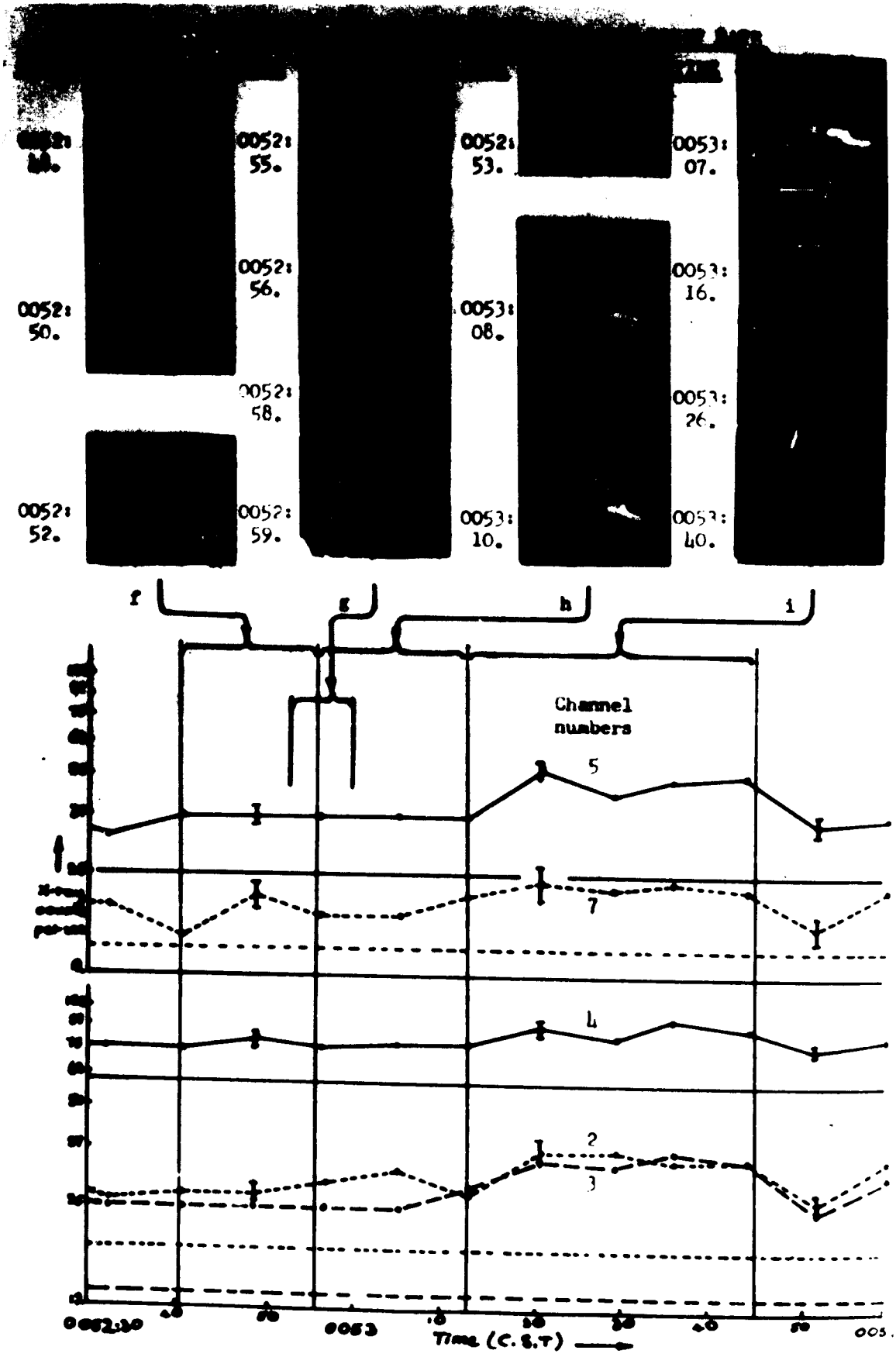
0052:
55.
0052:
56.
0052:
50.
0052:
58.
0052:
52.
0052:
59.
0052:
53.
0053:
08.
0053:
10.
0053:
07.
0053:
16.
0053:
26.
0053:
40.
f
g
h
i
Channel
numbers
5
7
4
2
3
0052:30
0053
Time (C.S.T)
005

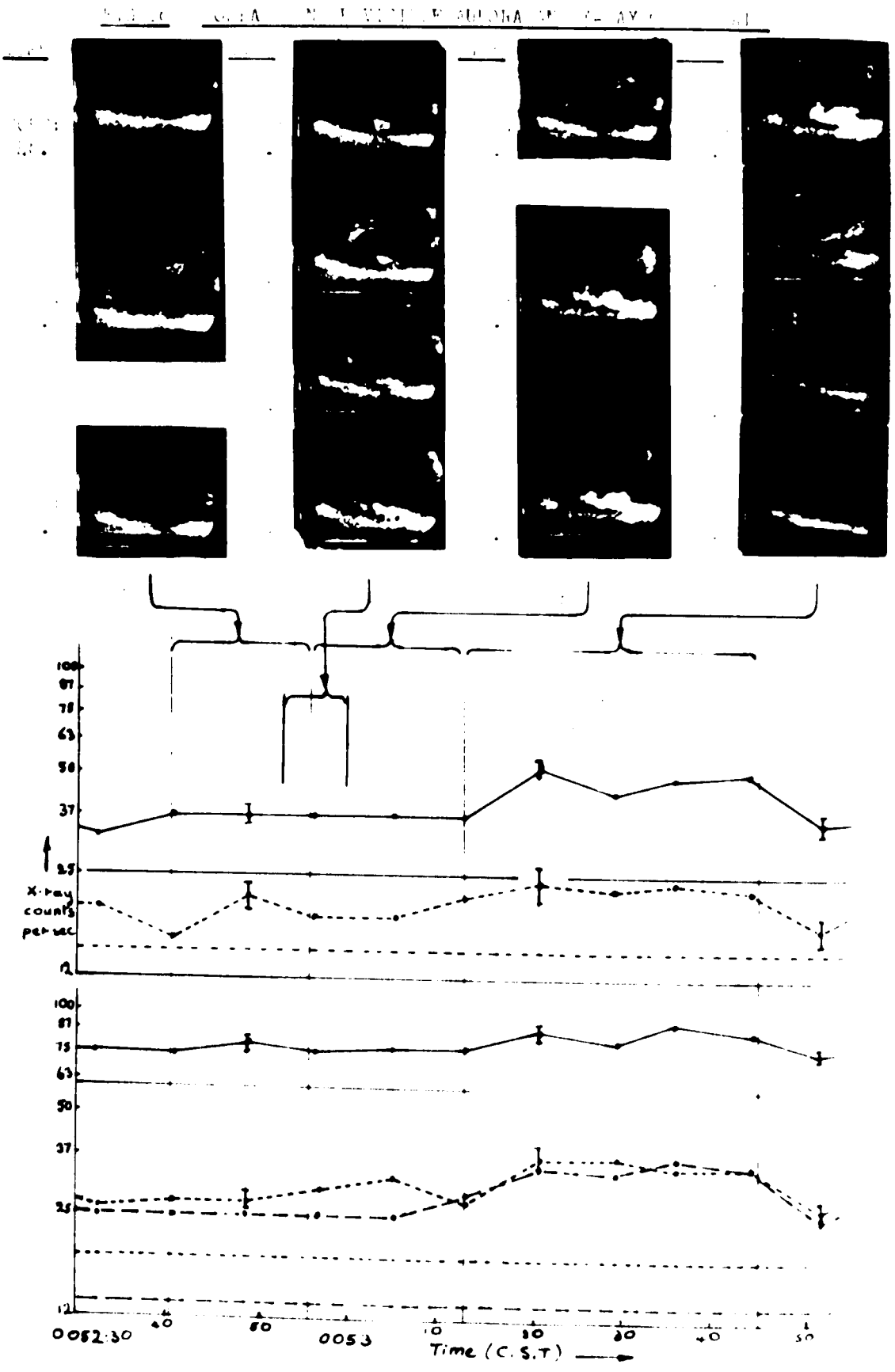
100
87
75
63
50
37
25
12
X-ray counts per sec
0052:30
40
50
0053
10
20
30
40
50
Time (C.S.T)

other bands in the same photographs appear single, it is more likely that the structure is genuine.

Event (f): Between 0052:44 and 0052:53 a diffuse patch appeared 40 km north of the balloon zenith (Fig. 16(f)). This patch showed a maximum intensity at about 0052:50. Channels 4 and 7 showed an increase in the x-ray counting rate about this time; the other channels remained constant. The increase in channel 4 amounted to about 6% (this increase is about equal to the probable error). Channel 7 increased by about 30% (twice the probable error). Only the latter of these count rate increases can be considered significant. This patch apparently was associated with a high energy flux of x-rays.

The white lines across the photographs for event (f) are caused by the oscilloscope horizontal line retrace. If intense luminosity was present at the eastern edge of the scan, the oscilloscope retrace was bright (no retrace blanking pulse was available).

Event (g): The peculiar double band seen in event (e) reappeared between 0052:53 and 0053:00 about 40 km northeast of the balloon zenith. The band, Fig. 16(g), extended westward and then swirled southward very rapidly. The estimated speed of the front end of this band is 10 (±50%) km/sec. No x-ray increases corresponding to these times were observed.

Event (h): From 0052:44 to 0053:11, moderately bright aurora was present in the east, Fig. 16(h). This was the end of a band stretching from east to west in the northern sky. Between 0052:44 and 0053:05 the band increased steadily in intensity and moved slowly overhead, to about 60 km north of the balloon zenith. From 0053:05 to 0053:11 the band diminished rapidly.

The appearance of this band is associated with an increase of x-rays in channel 2, which occurred between 0052:50 and 0053:06, and the sudden decrease again at 0053:13. The increase in channel 2 amounted to about 20% (an increase of twice the probable error). None of the other x-ray

channels showed an increase of counting rate at this time. This band was apparently associated with a very low energy flux of x-rays.

Event (i): The bright band of aurora, in the lower center of the second and third photographs shown for event (h) above, is the result of the activity in event (g) and is estimated to be about 70 km south of the balloon zenith.

Between 0053:13 and 0053:20 this band decreased in intensity but moved north to about 20 km from the balloon zenith, Fig. 16(i). After 0053:20 the aurora decreased steadily in intensity until 0053:42, at which time just an arc was visible on the southern horizon and faint aurora overhead.

An increase in all x-ray energy channels corresponds to the movement of the aurora towards the balloon. The increases amounted to about twice the probable error in all channels.

After 0053:20 the x-rays remained approximately

constant then dropped sharply between 0053:45 and 0053:50. These changes do not fit the observed auroral changes. However, active aurora was present overhead at Fort Churchill at this time (visual report). This was outside the scanner field of view and about 100 km from the point above the balloon.

The scanner was not in operation between the times 0053:45 and 0054:10.

Event (j): At 0054:10 the scanner resumed operation. At this time a bright patch of aurora, Fig. 17(j), was present due west, and a bright band (Type B red) was present at a position about 30 km south of the balloon zenith. It appears that this activity was responsible for the increase in x-ray flux observed in all channels after 0053:50.

The band in the south died out by 0054:18 correlating with a drop in x-ray channels 2, 4, 5 and 7 about this time. Only the decrease in channel 2 was greater than the probable error in the count rate. Note that this represents

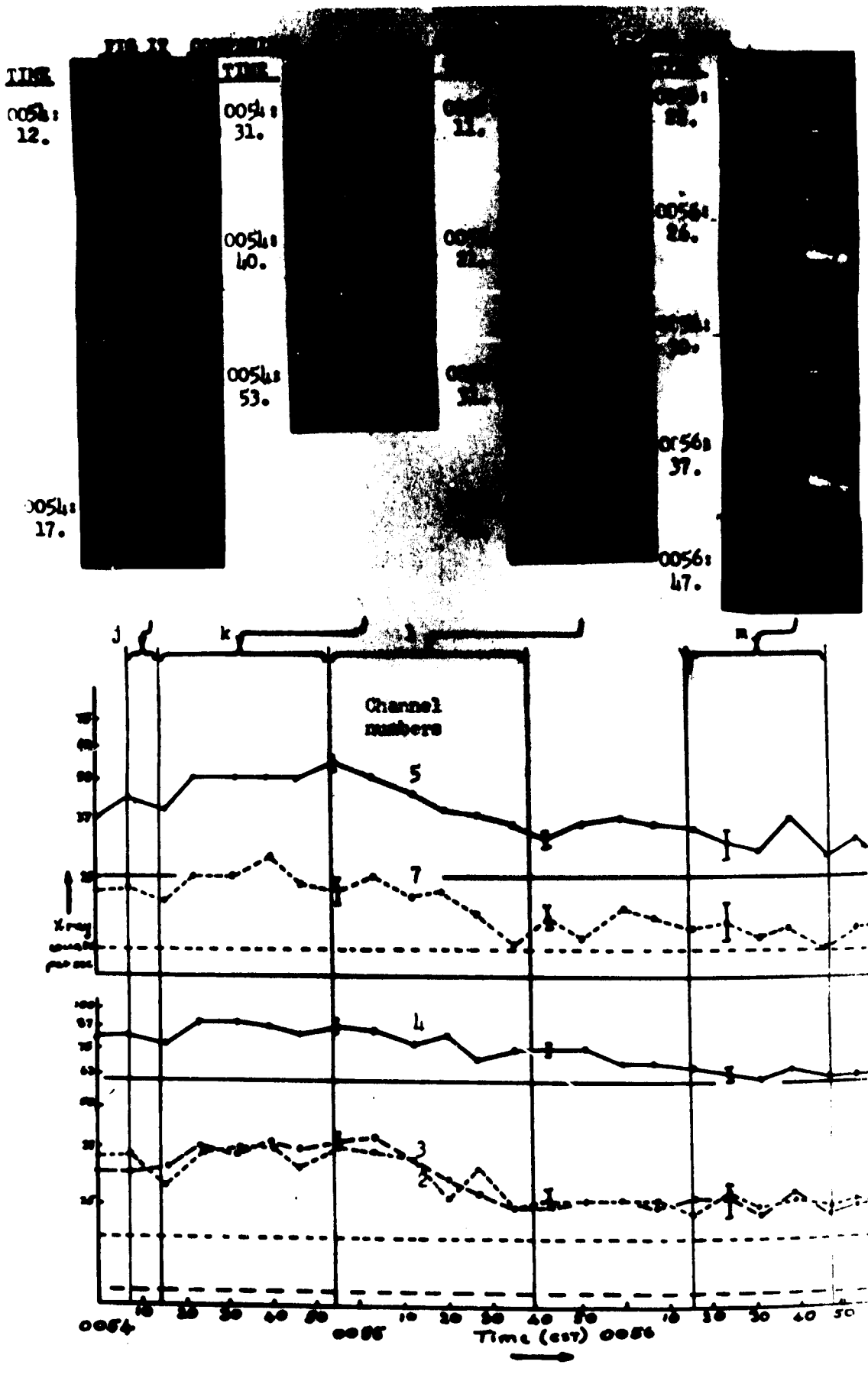
TIME
0054:
12.
TIME
0054:
31.
0054:
40.
0054:
53.
0054:
17.
0056:
37.
0056:
47.
J
k
m
Channel
numbers
5
7
4
3
2
X-ray
0054
0055
Time (EST) 0056

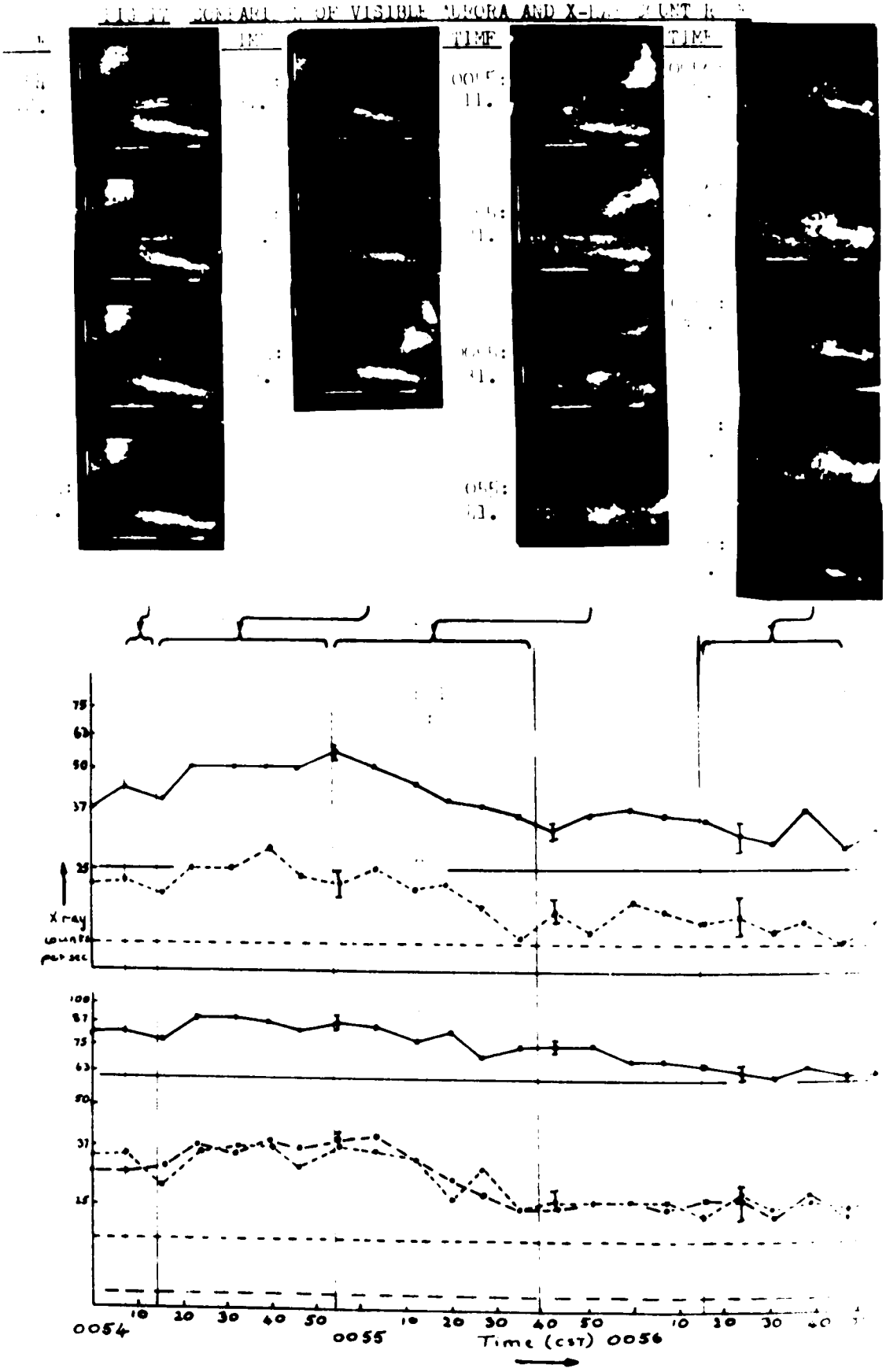
X ray
counts
per sec
0054
0055
Time (CST) 0056

the third appearance of a thin double band in this general region.

Event (k): At 0054:15 the x-ray counting rate suddenly increased in all channels by about twice the probable error. This cannot be correlated with any aurora in the scanner field of view, but, according to the A.S.C. data, a bright band (Type B as reported by observer) stretched across the northern sky.

At 0054:30 the eastern end of the band, mentioned above, appeared in the scanner field of view, Fig. 17(k), moving steadily towards the balloon and brightening. During this interval the x-ray intensity remained high but showed no further increase.

Event (l): From 0055:00 to 0055:40 the auroral band described above (still Type B red--visual report) continued to brighten and move further southand west, directly over the balloon, reaching a maximum at 0055:20. During this time, the x-ray counting rate showed only a steady decrease.

From 0055:20 to 0055:40 the band rapidly died away leaving faint diffuse aurora over most of the scanner's field. This is shown in Fig. 17(l).

Between 0055:40 and 0056:20, active and bright aurora could be seen in the zenith and a quiet band to the south of the balloon. No significant variations were noted in the x-ray count rate for this period; however, the auroral activity was low compared to the events discussed.

Event (m): At 0056:26 the band brightened, Fig. 17(m), at about 50 km to the south of the balloon. At 0056:30 it dimmed; 0056:37, brightened again; and at 0056:47, dimmed and slowly disappeared.

These variations in auroral intensity can be associated with similar variations in the x-ray counting rates in all the five channels shown. The times of the auroral fluctuations are not identical to the times of the corresponding changes in the x-ray data, but are within the estimated 5-second error. The variations are less than the

statistical error in all channels; however, all five channels increase and decrease at the same time, except that channels 4 and 5 do not show the first peak. (The probability of three channels varying together by as much as the probable error in each channel, due to statistical fluctuations alone, is less than 10%.)

Summary

Out of the thirteen single events considered, it was possible on nine occasions to obtain correlations between the visible aurora seen in the scanner photographs and x-rays detected by the balloon instrument. The first three events show definite correlations, the remaining six are not quite as obvious but do show similar time-coincident variations of x-ray counting rate and auroral intensity. Much more data would have to be analysed before any definite conclusions could be drawn.

In several cases the x-ray graph of counting rate against time suggests that consecutive x-ray events overlap. The slow increase and decrease

of counting rate can be associated with the aurora moving toward or away from the balloon, or changing in intensity.

X-rays have been found associated with most types of auroral forms, the largest x-ray fluxes being associated with the brightest and most active forms, which usually exhibited Type P red color.

If event (i) is considered reliable, it appears that proximity of the aurora causes more effect on the counting rate than intensity changes. In this event the aurora decreased in intensity and moved closer to the balloon, resulting in an increase in x-ray count rate.

Event (g) is unusual in several respects. It appeared as a very rapidly moving band. The speed of this form was much greater than that of others, however, the band was only of intensity I or II and swirled south at about 60 km from the balloon. This low intensity and relatively large distance could account for the failure to detect associated x-rays.

Fig. 18: X-ray Energy Spectrum (background).

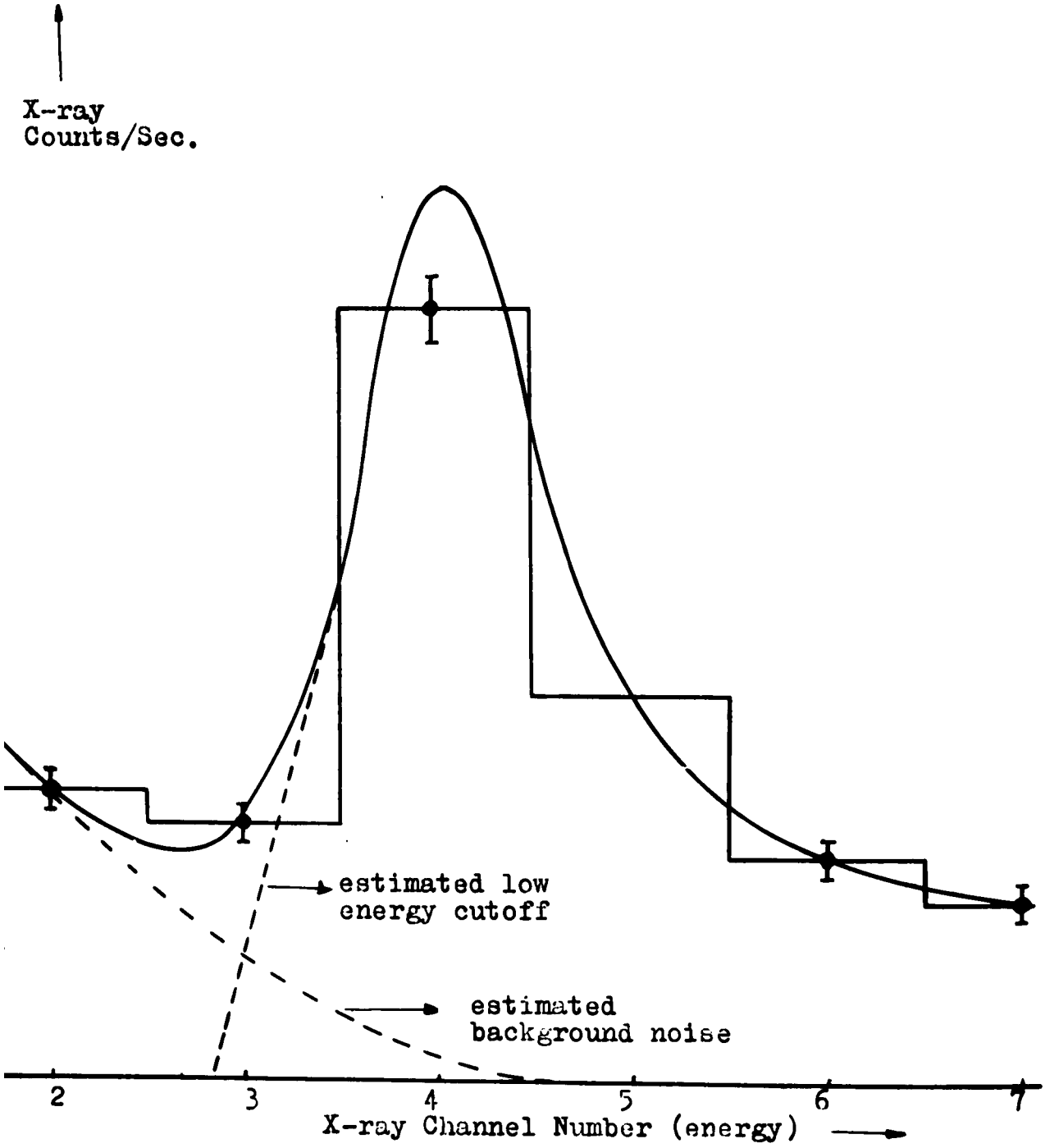

Events (k) and (l) appeared as relatively fast moving forms. The band, showing Type B red, moved from the east to the southwest, directly over the balloon at about 1 km/sec. (This is slow compared to the other events considered but fast compared to the usual speed of bands according to Chamberlain (1961). The band could definitely be associated with x-rays, as the counting rate remained high during this event. The drop off of x-rays, as the band appeared to brighten, cannot be explained. Other aurora, outside the scanner field, may have caused the initial maximum in the x-rays and the drop off of counting rate.

(iii) Analysis of X-ray Energy Spectrum

Fig. 18 is a typical x-ray spectrum, uncorrected for background, corresponding to the latter part of the event discussed. At these counting rates, which are little higher than the x-ray cosmic ray background, a terrestrial noise

signal is apparent in channel 2. The spectrum should fall off rapidly at low energies, due to atmospheric absorption of the x-rays.

The spectra obtained were in the form of histograms; however, the following analysis will be clearer if continuous smooth curves are drawn through the points as shcwn.

For the following spectra the counts were not corrected for background, as it was not known with sufficient accuracy. However, the analysis is independent of any background correction, assuming it did not change during the event. This assumption appears valid, as the spectra before and after the events are similar.

The approximate energy ranges of the x-ray channels are given in the Appendix. Because of the large errors and the numerous other faults with the data it was considered pointless to attempt to extrapolate the x-ray flux back to zero atmosphere to obtain the initial x-ray spectrum.

Fig. 19. X-Ray Energy Spectra

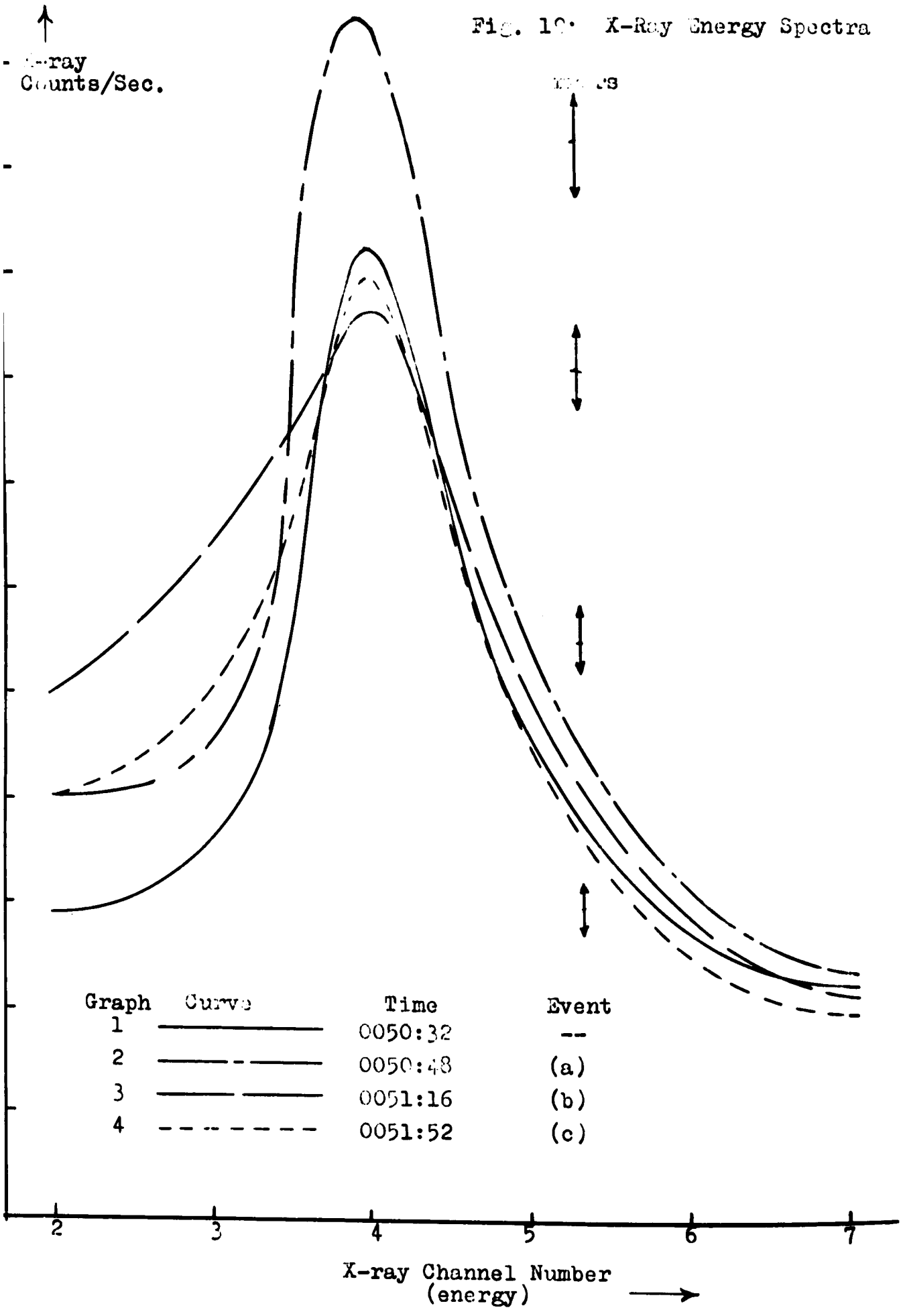

Fig. 19 shows the only four examples of the x-ray spectrum where the count rate was sufficiently high that the terrestrial noise signal could be considered insignificant and the spectral changes significant. The errors shown are standard deviations plus a conservative data reading error of ± 1 count/sec in all channels.

Graph 1 shows the x-ray spectrum prior to events (a), (b) and (c) (see preceding analysis).

Graph 2 represents the x-ray spectrum during event (a). Channel 2 has increased by 30%; channels 3 and 4 by 25%; and channels 5 and 7 by 20% and 5%, respectively.

Graph 3 represents the spectrum during event (b). Channels 2 and 3 have increased by about 70% and 80%, respectively, whilst channels 4, 5 and 7 have increased by only 1%, 12% and 0%, respectively. All increases are taken relative to graph 1.

Graph 4 represents the spectrum during event (c). Channels

2 and 3 have increased by 33% and 27%, respectively, whilst channels 4, 5 and 7 only increased by 0%, 0% and 10%, respectively. Increases again are taken relative to graph 1.

Between events (b) and (c) the spectrum dropped at the lower energies and was identical to graph 1 shown. Any variations of less than 10% can be ignored due to errors.

Tabulating the above --

Event	Distance From Balloon (km)	Intensity	Color	Channel No. (% increase) 2	3	4	5	7
(a)	60	II$^+$ or III	Type B(red)	30	25	25	20	0
(b)	40	III	Type B(red)	70	80	0	0	0
(c)	0	II or III	Type B(red)	33	27	0	0	0

Discussion of Spectral Data

The observed changes in the x-ray spectra must be associated with a change in the primary electron spectrum and cannot be explained by the variation in the distance between aurora and balloon.

The aurora during events (b) and (c) came closer to the balloon than during event (a) and, as expected, relatively more low energy x-rays were detected. The auroral luminosity and the number of high energy x-rays were essentially the same for events (b) and (c). As the aurora in event (b) did not come as close to the balloon as in event (c), a much sharper low energy cut-off would be expected for (b). This, however, was not the case and so the noted spectral change must have resulted from a spectral change of the primary electrons.

It is very likely that the maximum of the spectrum occurs at a lower energy for events (b) and (c) than for event (a). This is not obvious from the graphs shown because of the lack of energy resolution. If the estimated background spectrum (the lowest counts in each channel for the 8-minute period considered) is subtracted from the x-ray counts, the maximum point of the spectra changes from channel 4 to channel 3 for events (b) and (c) only.

CHAPTER 5

CONCLUSION

The following conclusions were drawn from the analysis of the scanner photographs of visible aurora and the x-ray data, from balloon borne equipment, obtained on the night of April 21st to 22nd, 1964.

1. X-rays showed a detailed association with visible aurora for nine of the thirteen events which occurred during an 8-minute display of visible aurora. On three occasions the observed auroral changes were quite different from the noted x-ray changes and on one occasion active visible aurora was observed with no x-rays detected.

2. On four other occasions during the same night, x-rays were detected time coincident with the observation of faint, inactive visible aurora.

3. In general, more active and bright aurora were associated with the largest x-ray fluxes. Proximity of the aurora showed a definite relationship to increases in the x-ray flux.

4. During the most active periods, the observed spectral changes are contrary to what would be expected if due entirely to variations of the atmospheric depth between the aurora and x-ray detector. The changes must, therefore, be associated with a change in the primary electron spectrum.

It must be emphasized that the data analysed, particularly the scanner photographs, are extremely flexible. (A correlation, between aurora and x-rays, was obtained even with incorrect timing of the scanner photographs. This was not as detailed as the correlation obtained with the correct timing). Consequently, many more events would have to be analysed before any definite conclusions could be drawn.

This analysis shows the usefulness of fast auroral photographs, compared to the necessarily long time exposures required by film and the uncertainties associated with verbal reports. The verbal reports used in this analysis were found to be inadequate to identify specific auroral forms during the breakup but were useful for identifying the color

of the form, in particular the presence of Type B red aurora.

A recent modification to the scanner is the inclusion of a filter changer. The filters can be changed from a narrow band 5577 $\mathring{A}$ filter to a wide band filter for the N_2 first positive bands responsible for the Type B red color.

The auroral photographs were found to be adequate for the analysis in this thesis but would be inadequate for the investigation of very fast motions, very dim forms, or rayed structures where an angular resolution of better than 1^o is required.

The scanner described provides much better sensitivity than film (a factor of about 30) and a wide field of view, producing a picture very similar to that which would be seen by an observer looking at the same region of the sky.

Another significant advantage of this type of instrument is that it permits the direct use of a narrow band

interference filter. The system provides sufficiently good rejection of background light that investigation of dim aurora during twilight is possible.

The mechanical and electronic parts were relatively simple in design and construction, but the former was not as reliable as desired, particularly at the lower temperatures encountered in Fort Churchill. However, a number of mechanical and electrical improvements have since been made which should result in substantial improvements in performance and reliability. The plane mirror, which oscillated with linear angular velocity, has since been changed so as to oscillate with simple harmonic motion. This will provide a longer dwell time at the extreme of the mirror motion, which is desirable for operation of the oscilloscope camera. This will introduce slight brightness but not space distortion of the final picture.

Sensitivity at very low light levels has been improved by the use of very high gain pulse amplifiers in

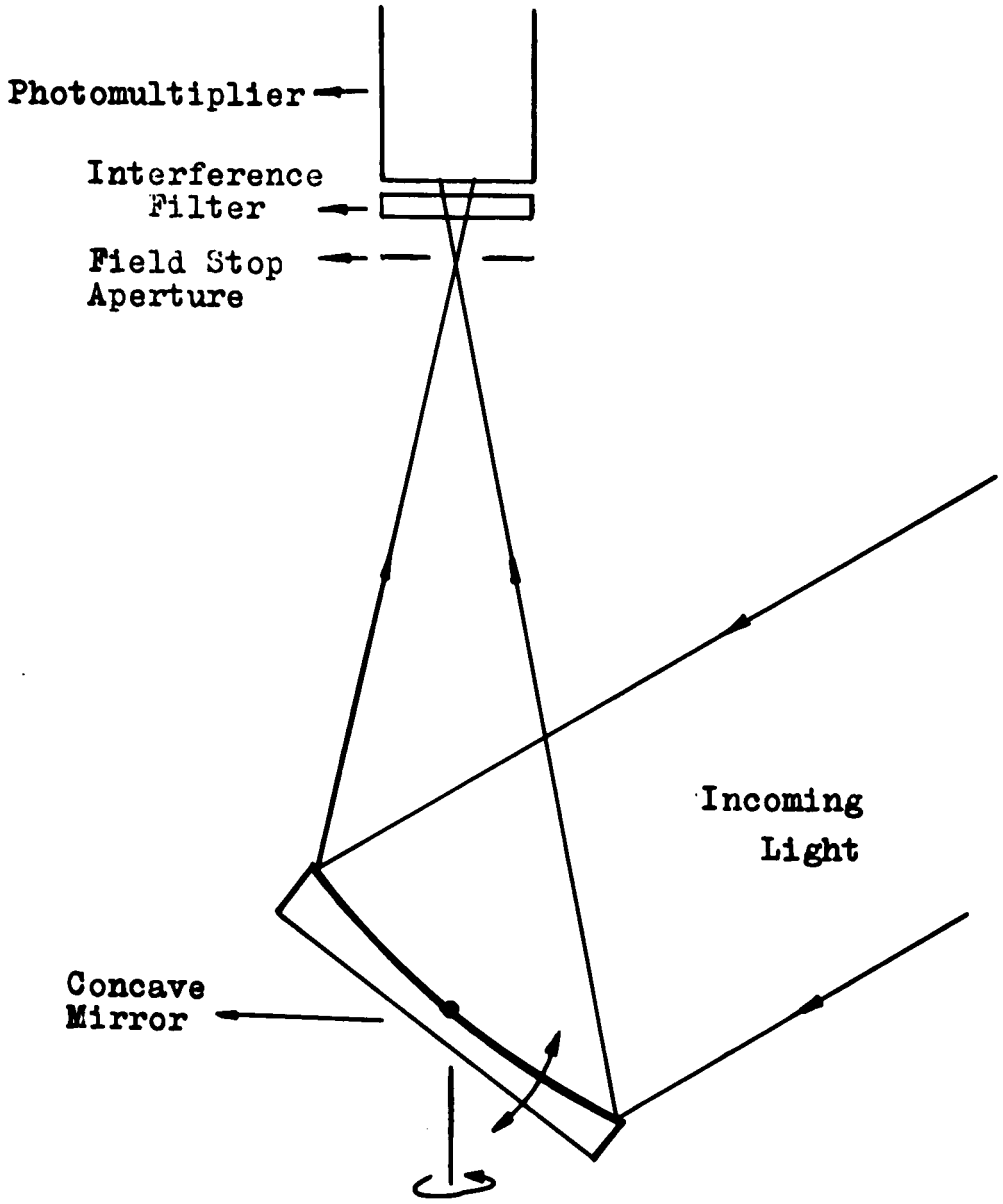

Fig. 20: Improved Spiral Scanner

the detector circuit in place of d.c. amplifiers (Chapter 2, Section (ii)a).

From the foregoing analysis many of the deficiencies of the present scanner have come to light, in particular its low optical efficiency due to the large number of mirrors which are necessary with this particular system. Another deficiency is the inadequate field of view.

The following design, shown in Fig. 20, is suggested as an improvement over the equipment described. A 6" or 12" diameter concave mirror oscillates slowly about a horizontal axis and spins very rapidly about a vertical axis. This will produce a spiral scan similar to that of the device described in Chapter 2, Section (ii)a.

Such a system would provide a larger light receiving area and fewer optical components than the present scanner giving greater sensitivity. It also provides an all-sky field of view. However, with this system, space resolution

would have to be sacrificed to obtain fast photographs, purely from mechanical limitations.

APPENDIX

X-Ray Detector

The x-ray detector consisted of a NaI(Tl) scintillator optically coupled to a photomultiplier (Harshaw, Integral Line Type 4S4).

The current pulse from the photomultiplier, produced by an x-ray undergoing photoelectric absorption in the scintillator, is amplified and used to generate a rectangular pulse of constant length (about 25 μS). The amplitude of the pulse is proportional to the initial x-ray energy. The balloon transmitter is frequency modulated by the rectangular pulse. The received pulse is fed into a ten-channel pulse height analyser. The output of each channel drives a ratemeter which deposits a fixed charge onto a capacitor. The capacitor charge corresponds to the number of pulses counted in the particular energy channel. The charge on each capacitor is sampled each second, and the charge and corresponding channel are

displayed on an oscilloscope. The resulting histogram shows the x-ray energy against the number of counts at each energy. After a period of time, depending on the x-ray count rate, the analyser channels are reset. The histograms and a clock are photographed.

With such a system an inflight calibration is essential. In this equipment, calibration is effected by setting the range of pulse heights (x-ray energies) over which the system operated. The histogram, produced by the pulse height analyser, should thus cut off sharply at some known upper and lower x-ray energy levels. Unfortunately, the lower level could not be defined due to local terrestrial noise and the upper level could not be defined, as no pulses were of sufficient energy to fill the channel just below the upper cutoff. Thus, the x-ray energy levels shown in the histogram could only be estimated.

To rectify this problem in future balloon flights, the balloon packages will contain a small radioactive

Fig. 21: Example of X-ray Data

source which emits x-rays of known energy. Peaks corresponding to these energies should be obvious on top of the background x-ray spectrum at low counting rates.

Fig. 21 shows the series of histograms obtained from the x-ray detector.

Each vertical column of lines corresponds to a different x-ray energy channel. The height of a particular line corresponds to the total accumulated number of counts in that channel. The lowest line in each channel corresponds to the number of counts in that channel after one second. The next lines show the accumulated counts after two seconds and so on up to eight seconds. After eight seconds the channels are reset to zero counts.

The number of counts in each channel could be read off the photograph, using a calibrated scale (with an estimated reading error of about 10 counts). Channels 1 to 5 could count to a maximum of 1000 counts in the eight seconds, and channels 6 to 10 only 250 counts for the same vertical

deflection. (The number of counts in channels 1 to 5 were expected to be much greater than the counts in channels 6 to 10.)

The energy range per channel was estimated to be --

Channels 1 and 2	Noise	Estimated error
3	15 to 30 KeV	±50%
4	30 to 45	
5	45 to 60	
6	60 to 75	
7	75 to 90	
8	90 to 105	
9	105 to 120	
10	120 to 135	

Channels 9 and 10 showed no counts. This could be because these channels corresponded to energies above the upper level discrimination in the balloon instruments, but it is more probable that a negligible number of x-rays at these energies were present.

LIST OF REFERENCES

Anderson, K.A., 1958. Phys. Rev. Vol. III. 1397 - 1605.

Anderson, K.A. and Enemark, D.C., 1960. J. Geophys. Res. Vol. 65, No. II.

Anderson, K.A., 1961. International Conference on the Earth Storm and Cosmic Rays, Kyoto, Japan.

Anderson, K.A. and Dewitt, 1963. J. Geophys. Res. Vol. 68, No. 9.

Chamberlain, J.W., 1961. Physics of the Aurora and Airglow, Academic Press.

Chapman, S., 1961. International Conference on the Earth Storm and Cosmic Rays, Kyoto, Japan.

Davis, T.N. and Hicks, G.T., 1964. J. Geophys. Res. Vol. 69, No. 9.

Davis, T.N. and Hicks, G.T., 1965. Applied Optics, Vol. 4, No. 2.

Farnell, G.C. and Chanter, J.B., 1961. Journal of Photographic Science, Vol. 9.

Gartlein, C.W., 1947. Nat. Geog. Magazine, Nov.

Goetze, G.W. and Boeris, A.H., 1964. Proc. I.E.E.E. Vol. 52, No. 9, Sept.

Holten, M.R. and Wolfe, W.L., 1959. Proc. I.R.E. Vol. 47, No. 9.

Lebedinskii, A.I., 1955. Doklady Akad. Nauk S.S.S.R. Vol. 102.

McFee, R.H., 1959. Proc. I.R.E. Vol. 47, No. 9.

Montalbetti, R., 1957. Can. J. Phys. Vol. 35, No. 3

Morton, A., 1964. Applied Optics, June.

O'Brien, B.J. and Taylor, H., 1964. J. Geophys. Res. Vol. 69, No. 1.

Spalding, J.F. and Anderson, J.E., 1963. Application of Electro Optics to Auroral Studies. G.E. Company, Contract No. AF19(628) - 2366, Proj. No. 8563.

Struve, O., 1951. Sky and Telescope, July.

Winkler, J.R. and Peterson, L., 1957. Phys. Rev. Vol. 108, No. 11.

Winkler, J.R. et al, 1958. Phys. Rev. Vol. 110, No. 6.

Winkler, J.R. et al, 1959. J. Geophys. Res. Vol. 64, No. 6.